Simultaneous Assessment of the $YBa_2Cu_3O_{6+z}$ Thermodynamics Under the Linear Error Model

E. B. Rudnyi,[a] V. V. Kuzmenko, and G. F. Voronin

Chemistry Department, Moscow State University, 119899 Moscow, Russia

Received October 22, 1997; revised manuscript received April 7, 1998

About 3000 experimental points obtained in 220 miscellaneous experiments published in 57 papers have been processed simultaneously in order to obtain the most reliable Gibbs energy of the $YBa_2Cu_3O_{6+z}$ solid solution in the temperature range from 250 to 1300 K. A part of this solution is well-known as the "Hi-T_c Y123" phase. All other thermodynamic properties of the solution including the conditions for the tetragonal-orthorhombic phase transition and the miscibility gap at lower temperatures, are derived from the assessed Gibbs energy. The linear error model introduced recently by one of the authors has been employed for the simultaneous assessment. The results obtained are compared with those of the conventional weighted least squares method and the benefit of the new approach is discussed. Another problem in simultaneous assessment that is also considered is visualizing the quality of the fit. New types of graphs (partly based on the linear error model) that facilitate visualizing the quality of the fit are presented. (A critical review with 72 references.) [S0047-2689(98)00404-8]

Key words: Chemical thermodynamics; enthalpy of formation; entropy; Gibbs energy; heat capacity; high-temperature superconductor; lattice model; maximum likelihood; mixed model; variance component; visualizing quality of the fit.

Contents

List of Tables

List of Figures

[a]Electronic mail: rudnyi@comp.chem.msu.su

1. Introduction

The $YBa_2Cu_3O_{6+z}$ phase is the first material that has been found to be superconducting above the liquid nitrogen temperature and is often referred to as the "Hi-T_c Y123" phase (see 87WU/ASH). Its properties have been studied in many laboratories, and numerous experimental values are currently available. Nonstoichiometry index z can change from zero to one, and thermodynamically speaking, this phase is considered to be a solid solution. In the present work the terms "phase" and "solid solution" will be assumed to be interchangeable. The $YBa_2Cu_3O_{6+z}$ phase was found to exist in two modifications, tetragonal and orthorhombic, and only the latter happened to be a superconductor.

The goal of the present study is to compile all the experimental values related to the thermodynamic properties of the $YBa_2Cu_3O_{6+z}$ solid solution and to assess the most reliable Gibbs energy as a function of temperature and nonstoichiometry index z. When the Gibbs energy of the solid solution is known, all the other thermodynamic properties can be obtained by means of the thermodynamic laws.

The lower temperature of the assessment has been limited by 250 K (see Sec. 2). This means that in the present work the superconducting region by itself is not considered. The importance of the results obtained is rather tied with further possibilities to find out the chemical composition, the temperature, the oxygen pressure and other conditions for the synthesis of the superconductive phase.

The present work is the continuation of 93VOR/DEG (see also 90DEG, 90DEG2, 90MER/DEG, 91VOR/DEG) where a thermodynamic model of the $YBa_2Cu_3O_{6+z}$ phase has been suggested and the Gibbs energy has been already estimated. In the present work, new experimental results that have appeared recently have been included in the assessment, and more attention has been paid to the statistical treatment.

We are aware of other papers that have been devoted to the assessment of the $YBa_2Cu_3O_{6+z}$ phase thermodynamics since 1991 (discussion of the previous attempts can be found in 91VOR/DEG). However, in our view, none of them has reached the final goal of providing a reliable estimation of the Gibbs energy.

The $YBa_2Cu_3O_{6+z}$ thermodynamic model in 91LEE/LEE treats this compound as a single phase, and hence the results of 91LEE/LEE do not allow us to distinguish between the $YBa_2Cu_3O_{6+z}$ orthorhombic and tetragonal modifications. This is very unfortunate because only the orthorhombic phase possesses superconducting properties, and thus all the practitioners would like to know which modification will be formed under given conditions.

93PLE/ALT have assessed the thermodynamic properties of the $YBa_2Cu_3O_{6+z}$ phase by means of a step-by-step approach. This means that they evaluated the heat capacity, the enthalpy, oxygen partial pressure, and other properties consecutively without employing any uniform model. As a result, the equations given do not obey the thermodynamic laws. For example, Eq. (12) in this article contradicts Eqs. (9) and (11), i.e., according to the thermodynamic laws these equations cannot be held simultaneously true.

Recently 96BOU/HAC have published a paper where they have claimed that an assessment of $YBa_2Cu_3O_{6+z}$ phase thermodynamics has been accomplished (none of Degterov and Voronin's work has been cited). Unfortunately, all that is available there is a sentence "we did it." In order to discuss this claim we have to wait until more details are published.

For a given system, the more experiments that are conducted, the more reliable the results. No one seems to argue with this statement. On the other hand, however, the results of the distinct experiments usually differ more between each other than the reproducibility error in a single experiment. In this respect, the $YBa_2Cu_3O_{6+z}$ phase is a very good example because we do have a lot of data that have been published since the material has been discovered: more than 3000 experimental points obtained in about 220 experiments conducted by nearly 50 laboratories. Nevertheless, as one may

expect, the scatter of the results is rather huge, and mere fitting of all the results makes no sense at all.

The quality of different experiments is certainly different, and moreover, the quality of the resulting presentation is also different. For example, many authors have presented their experimental results as figures only. With the advent of the digital scanners, it is relatively easy to convert these figures to numbers, but the question as to how accurately these figures have been made remains unanswered.

Traditionally, the question of the data quality has been solved by means of weighted least squares (WLS), where an expert assigns a weight to each experimental point *a priori* based on her or his preferences. The main problem by this technique is the relative subjectivity. It is relatively easy to say that the weight for this point should be equal to one, and for that point to be equal to one and half. It is not that easy though to explain how one comes to that conclusion. It should be especially mentioned that we are not against subjectivity. Whether we want it or not, subjectivity can never be completely excluded in practical applications. Hope for the "golden" algorithm that would just take raw data and produce the true answer is unrealistic because, before processing data, we must always postulate some hypothesis that cannot be proved empirically in that treatment.

Still, subjectivity can be put under stronger control than in the case of WLS, as has been shown by 96RUD, 97RUD, and 97KUZ/USP. The new advanced methods of mathematical statistics allow an expert to make the qualitative conclusions only and let the formal methods do the rest. Making qualitative statements is much easier for the human being, and furthermore, this division also leads to a formal way of expressing the qualitative conclusions that are necessary for a simultaneous assessment.

Thus, the goal of the present work is twofold: first, to obtain the most reliable Gibbs energy of the $YBa_2Cu_3O_{6+z}$ solid solution; second, to discuss the new approaches for a simultaneous assessment using this example. We will start with the description of the thermodynamic model of the phase in Sec. 2 and available experimental results in Sec. 3. Then, in Sec. 4, we will review the linear error model (see 96RUD and 97RUD for details) and describe its application to the thermodynamics of the $YBa_2Cu_3O_{6+z}$ phase. Section 5 is devoted to another important question in the simultaneous assessment: the visual comparison of different solutions. In Sec. 6, the results obtained are compared with those in WLS. Finally, Sec. 7 summarizes the methodological results that, in our view, have been achieved by the present study.

2. Thermodynamic Model

A thermodynamic model of the $YBa_2Cu_3O_{6+z}$ solid solution has been developed earlier by Voronin and Degterov in 90DEG, 90DEG2, 90MER/DEG, 91VOR/DEG and 93VOR/DEG. Below, there is just a brief review and 91VOR/DEG should be consulted for a complete description of the model.

The $YBa_2Cu_3O_{6+z}$ phase has a layered structure, $(CuO_2)(BaO)(CuO_2)(Y)(CuO_2)(BaO)$ of the perovskite type. Only one of the three copper-based layers, the so called basal plane, is responsible for the oxygen nonstoichiometry (adsorption, desorption and ordering). All other layers are considered to be stoichiometric and the overall formula unit can be written as

$$[Y^{+3}(Ba^{+2})_2(Cu^{+2})_2(O^{-2})_6](Cu^{+1},\ Cu^{+3})_1^{(m)} \times (O^{-2},\ Va)_1^{(a)}(O^{-2},\ Va)_1^{(b)}. \quad (1)$$

Here the basal plane is considered to comprise three sublattices: a cation sublattice for copper and two anion sublattices filled with the ions of oxygen and vacancies (Va). It was necessary to introduce two oxygen sublattices because the $YBa_2Cu_3O_{6+z}$ phase was found to exist in two modifications, tetragonal and orthorhombic. The occupancies of the sublattices (a) and (b) are the same in the tetragonal form, and the sublattice (b) is richer in oxygen in the orthorhombic form.

The sublattice model leads to the expression for the phase Gibbs energy as follows (complete calculations are given in 91VOR/DEG):

$$\begin{aligned}\Delta_{ox}G(T,z,x) = {} & g_1(T)+g_2(T)z+z(1-z)\Sigma_i a_i(T)(1-z)^i \\ & +(c^2-x^2)\Sigma_i b_i(T)(1-z)^{i-1}+T[(c+x) \\ & \times\ln(c+x)+(c-x)\ln(c-x)+(1-c+x) \\ & \times\ln(1-c+x)+(1-c-x)\ln(1-c-x) \\ & +z\ln z+(1-z)\ln(1-z)], \end{aligned} \quad (2)$$

where z is the stoichiometry index of the basal plane ($0 \leq z \leq 1$), c is short for $z/2$, x is the order parameter ($0 \leq x \leq z/2$), $g_i(T)$, $a_i(T)$, and $b_i(T)$ are temperature functions to be determined. $\Delta_{ox}G$ stands for the Gibbs energy of formation from the oxides, Y_2O_3, BaO, CuO, and oxygen, i.e., the Gibbs energy of the reaction

$$0.5Y_2O_3+2BaO+3CuO+(0.5z-0.25)O_2 = YBa_2Cu_3O_{6+z}. \quad (3)$$

The thermodynamic properties of the oxides and oxygen employed in the present work are listed in Table I.

As was already mentioned, the model allows for differing occupations of oxygen sites in the two sublattices to accommodate the Gibbs energy for tetragonal and orthorhombic modifications. To this end, the order parameter x in Eq. (2) is defined as the difference between the oxygen occupancies y_O in the sublattices (b) and (a) as follows

$$x=(y_O^{(b)}-y_O^{(a)})/2=z/2-y_O^{(a)}, \quad (4)$$

where oxygen occupancy means the oxygen mole fraction in the corresponding sublattice. Thus, x should be equal to zero for the tetragonal phase and $0<x\leq z/2$ for the orthorhombic phase.

According to the model, oxygen occupancies are not known, and the parameter x is considered as "internal," that is, for all the thermodynamic functions at equilibrium, we have just two independent variables, the temperature T and the index z. The value of x at any given T and z can be

TABLE 1. Auxiliary thermodynamic properties of oxides employed in the present work (according to 97VOR/USP)[a]

Oxide	$\Delta_f H^\circ_{298}$ kJ mol^{-1}	A	B	C	D	E	F
Y_2O_3	−1919.4	−30 047.83	954.1052	−146.996	−2120.104	737 146.5	−12 441 857
BaO	−548.0	−5092.968	463.41195	−72.028	−1858.564	0	−9 963 433
CuO	−161.7	−5669.132	477.64762	−69.785	−1801.184	61 609	0
O_2	0	−1776.280	132.54252	−44.978	−1294.168	0	13 651 002

[a]The parameters from A to F allow us to compute $G-H^\circ_{298}$, the Gibbs energy of the oxide ($p^o=101\,325$ Pa) according to Eq. (21) in J mol^{-1} in the temperature interval from 250 to 1300 K related to the standard enthalpy of oxide at 298.15 K, all other thermodynamic properties of the oxide can be obtained by means of well-known thermodynamic relationships. A large number of significant digits in the parameters $A-F$ is given in order to cope with strong correlation among them.

determined by minimizing Eq. (2) over x, or by equating to zero the partial derivative of $\Delta_{ox}G$ with respect to x

$$(\partial\Delta_{ox}G/\partial x)_{T,z}=0. \tag{5}$$

This equation cannot be solved generally in the closed form but the solution is quite an easy task for modern numerical analysis. The only precaution that should be taken here is to choose the correct root of Eq. (5) that corresponds to the minimum of Eq. (2).

The internal variable x makes the model a bit unusual even though this is quite an ordinary approach for modern solution models. Equation (2) describes function $\Delta_{ox}G(T,z,x)$ in three variables in closed form. In practice, the function $\Delta_{ox}G(T,z)$ is required because, in the case of $YBa_2Cu_3O_{6+z}$, it is possible to control two external variables only. Then, the order parameter x is assumed to reach the equilibrium value x_{eq} and we have

$$\Delta_{ox}G(T,z)=\Delta_{ox}G\{T,z,x_{eq}(T,z)\}, \tag{6}$$

where the function $x_{eq}(T,z)$ represents the solution of Eq. (5). Because the solution of Eq. (5) is not available in the closed form, Eq. (6) can be considered to be an algorithm that suggests computing $\Delta_{ox}G(T,z)$ in two steps: first solving Eq. (5) numerically for the equilibrium value of x and then substituting the result in Eq. (2). It is worthy noting that the same formalism holds for other thermodynamic properties of the $YBa_2Cu_3O_{6+z}$ phase, for example $\Delta_{ox}H(T,z)=\Delta_{ox}H\{T,z,x_{eq}(T,z)\}$. The use of numerical methods changes nothing in principle. We can safely think that the function $x_{eq}(T,z)$ is completely known, and the only difference is that the calculations become unworkable without computers.

Let us stress once more that the lattice model that brought Eq. (2) forth gives a uniform description for both modifications of the $YBa_2Cu_3O_{6+z}$ phase. Provided all the parameters in Eq. (2) are known, the type of the phase at any given T and z is determined by the function $x_{eq}(T,z)$ that is doubtlessly defined by Eq. (2) itself. If the equilibrium value of x is equal to zero then we have the tetragonal phase, otherwise the orthorhombic phase is more stable. The phase border between the two modifications can be found by solving the following equation

$$(\partial^2\Delta_{ox}G/\partial x^2)_{T,z}|_{x=0}=0. \tag{7}$$

This equation allows us to compute the phase transition temperature at the given index z provided all the parameters for Eq. (2) are known. Again, in the general case, this can be done by numerical methods only.

In writing Eq. (2), we have neglected the influence of the hydrostatic pressure, i.e., the term $\int_{p^o}^{p}V_m\mathrm{d}p$ because it is usually small for condensed phases. In this expression, p^o is the standard pressure for which Eq. (2) is supposed to hold (in the present work $p^o=101\,325$ Pa). However, in our model, the Gibbs energy of the $YBa_2Cu_3O_{6+z}$ phase depends heavily on the partial pressure of oxygen in the surrounding atmosphere. If the gas phase is in equilibrium with $YBa_2Cu_3O_{6+z}$, then, according to the equilibrium criterion, the oxygen partial pressure must be equal to

$$\ln\{p(O_2)/p^o\}=2\Delta_{ox}G'_O/RT, \tag{8}$$

where $\Delta_{ox}G'_O$ is the partial Gibbs energy, i.e., the partial derivative

$$\Delta_{ox}G'_O\equiv\{\partial\Delta_{ox}G(T,z)/\partial z\}_T. \tag{9}$$

Taking into account Eq. (6) and the differentiation rule for a compound function we obtain

$$\Delta_{ox}G'_O=\{\partial\Delta_{ox}G(T,z,x)/\partial z\}_{T,x}+\{\partial\Delta_{ox}G(T,z,x)/\partial x\}_{T,z}\{\partial x_{eq}(T,z)/\partial z\}_T. \tag{10}$$

The second term vanishes because of Eq. (5) and the final partial Gibbs energy takes the next form

$$\Delta_{ox}G'_O=\{\partial\Delta_{ox}G(T,z,x)/\partial z\}_{T,x}. \tag{11}$$

In many experiments the oxygen partial pressure was fixed externally and then the index z should be considered as a function, $z\{p(O_2),T\}$. The latter is implicit in Eqs. (5), (8), and (11), which should be solved for z at given the oxygen partial pressure and temperature. Then, all the thermodynamic properties can also be estimated under such conditions. For example, the Gibbs energy can be computed as follows

$$\Delta_{ox}G\{p(O_2),T\}=\Delta_{ox}G\{T,z[p(O_2),T],x_{eq}(T,z[p(O_2),T])\}. \tag{12}$$

Certainly, we rely again on numerical methods here.

The $YBa_2Cu_3O_{6+z}$ phase can be considered as a two-component solution and the formation of a miscibility gap cannot be excluded. Actually there is evidence that a miscibility gap with an upper critical temperature should occur in the $YBa_2Cu_3O_{6+z}$ phase about room temperature. The criterion for complete miscibility requires Eq. (2), as a function of z at constant temperature, to be convex, or the partial Gibbs energy $\Delta_{ox}G'_O$ (and then the oxygen partial pressure) to monotonically increase with the growth of z. If at some temperature this is not the case, then a miscibility gap is present and its borders can be found by solving a system of the two equations for two unknowns, z' and z'' $(z' \neq z'')$

$$\Delta_{ox}G(T,z'') - \Delta_{ox}G(T,z') = \Delta_{ox}G'_O(T,z')(z''-z') = \Delta_{ox}G'_O(T,z'')(z''-z'). \tag{13}$$

All other thermodynamic properties of the $YBa_2Cu_3O_{6+z}$ phase can also be found provided the Gibbs energy [Eq. (2)] is known. Taking into account that $H = -T^2\{\partial(G/T)/\partial T\}_p$ and $S = -\{\partial G/\partial T\}_p$ and then, as for the partial Gibbs energy [see Eqs. (9)–(11)], we have

$$\Delta_{ox}H = -T^2\{[\partial\Delta_{ox}G(T,z,x)/T]/\partial T\}_{z,x}, \tag{14}$$

$$\Delta_{ox}S = -\{\partial\Delta_{ox}G(T,z,x)/\partial T\}_{z,x}. \tag{15}$$

The thermodynamic relationship $C_p = (\partial H/\partial T)_p$ leads us to the computational expression for the heat capacity

$$\Delta_{ox}C_{pz} = \{\partial\Delta_{ox}H(T,z,x)/\partial T\}_{z,x} + \{\partial\Delta_{ox}H(T,z,x)/\partial x\}_{T,z}\{\partial x_{eq}(T,z)/\partial T\}_z. \tag{16}$$

Note that the second term is not equal to zero here and that in the case of $YBa_2Cu_3O_{6+z}$ some other heat capacities can be also introduced (see 93VOR/DEG). Equations (15) and (16) give the entropy and the heat capacity of reaction (3). The absolute values can be also obtained as follows

$$S = \Delta_{ox}S + 0.5S_{Y_2O_3} + 2S_{BaO} + 3S_{CuO} + (z/2-0.25)S_{O_2}, \tag{17}$$

$$C_{pz} = \Delta_{ox}C_{pz} + 0.5C_{p,Y_2O_3} + 2C_{p,BaO} + 3C_{p,CuO} + (z/2-0.25)C_{p,O_2}. \tag{18}$$

Another thermodynamic property that has been measured for the $YBa_2Cu_3O_{6+z}$ phase is the partial enthalpy. After analogous considerations as above, it can be derived as follows

$$\Delta_{ox}H'_O = \{\partial\Delta_{ox}H(T,z)/\partial z\}_T = \{\partial\Delta_{ox}H(T,z,x)/\partial z\}_{T,x} - \{\partial\Delta_{ox}H(T,z,x)/\partial x\}_{T,z}\{\partial x_{eq}(T,z)/\partial z\}_T. \tag{19}$$

Therefore, if the values of all the parameters in Eq. (2) are known, then, each thermodynamic property of the $YBa_2Cu_3O_{6+z}$ phase is also known, and the assessment of $YBa_2Cu_3O_{6+z}$ thermodynamics is equivalent to determining the unknown temperature functions, $g_i(T)$, $a(T)_i$, $b_i(T)$ in Eq. (2). The latter determination is possible if we choose some analytical function in temperature and put unknown parameters within it. In this way, the traditional approach for solution thermodynamics was followed when the temperature function is based on the expression for the Gibbs energy of the stoichiometric compounds that in turn depends on the temperature dependence of the heat capacity. However, the form of the heat capacity function accepted in the present work,

$$C_p = k_0 + k_1T^{-0.5} + k_2T^{-2} + k_3T^{-3}, \tag{20}$$

does not enjoy widespread use yet. Equation (20) was invented by 85BER/BRO who have demonstrated its advantage as compared with traditional Maier and Kelley's and other equations for oxides. Provided k_1 and k_2 are not positive, Eq. (20) ensures that heat capacity approaches the high temperature limit predicted by lattice vibrational theory and thus this makes extrapolating the low-temperatures heat capacities to high temperatures rather reliable. According to 85BER/BRO, Eq. (20) can be safely used from 250 to 3000 K and this range sets the lower limit for the temperature interval in the present work. Equation (20) leads to the temperature dependence of the Gibbs energy as follows:

$$G(T) = A + BT + CT\ \ln T + DT^{0.5} + ET^{-1} + FT^{-2}, \tag{21}$$

where two additional parameters have appeared during two integrations. As a result, functions $g_i(T)$, $a(T)_i$, $b_i(T)$ in Eq. (2) are assumed to have the form of the right-hand side of Eq. (21), and the task of the assessment is to determine unknown parameters from A to F for each temperature function in Eq. (2).

3. Literature Experimental Values

In this section the experiments are classified according to the measured properties of the $YBa_2Cu_3O_{6+z}$ phase. For each group of experiments, a measured property and variables under control are considered first. As we neglected the hydrostatic pressure, the $YBa_2Cu_3O_{6+z}$ phase has two degrees of freedom and thus two variables should be controlled in any experiment. The only exception is in experiments for determining the line of the phase transition where, according to the Gibbs phase rule, the $YBa_2Cu_3O_{6+z}$ phase has one degree of freedom. A typical notation for the experimental point is

$$\{y_{ij}, u_{ij}, v_i\}, \tag{22}$$

where the index i enumerates the experiments, j denotes the experimental points within the ith experiment ($j = 1,\ldots,N_i$), y_{ij} is what has been measured, u_{ij} is what has been changed, and v_i is what has been fixed during this

TABLE 2. Experimental results available for the assessment of the $YBa_2Cu_3O_{6+z}$ phase thermodynamics

Code	Set of values	N_t	Inc.[a]	v_i[b]	Method[c]	Reference
TB1	$\{T_{ij}, \ln p(O_2)_{ij}\}$	5	+	n/a	XRD	87BRY/GAL
TE	$\{T_{ij}, \ln p(O_2)_{ij}\}$	2	+	n/a	XRD	87EAT/GIN
TF	$\{T_{ij}, \ln p(O_2)_{ij}\}$	10	+	n/a	Resistivity	87FIO/GUR
TK	$\{T_{ij}, \ln p(O_2)_{ij}\}$	5	+	n/a	TGA	87KUB/NAK
Ts	$\{T_{ij}, \ln p(O_2)_{ij}\}$	1	−	n/a	XRD	87SCH/HIN
TT	$\{T_{ij}, \ln p(O_2)_{ij}\}$	2	+	n/a	TGA, XRD	87TAK/UCH
TY	$\{T_{ij}, \ln p(O_2)_{ij}\}$	1	+	n/a	XRD	87YUK/SAT
To	$\{T_{ij}, \ln p(O_2)_{ij}\}$	2	+	n/a	XRD	88KOG/NAK
Tp	$\{T_{ij}, \ln p(O_2)_{ij}\}$	5	+	n/a	XRD	88SPE/SPA
Tu	$\{T_{ij}, \ln p(O_2)_{ij}\}$	4	+	n/a	XRD	88TOU/MAR
TW	$\{T_{ij}, \ln p(O_2)_{ij}\}$	4	+	n/a	XRD	88WAN/LI
TB2	$\{T_{ij}, \ln p(O_2)_{ij}\}$	1	+	n/a	XRD	89BRY/GAL
TM1	$\{T_{ij}, z_{ij}\}$	7	−	n/a	Resistivity	88MEU/RUP
TM2	$\{T_{ij}, z_{ij}\}$	13	−	n/a	Resistivity	89MEU/NAE
XJ0	$\{x_{ij}, T_{ij}, \ln p(O_2)_i\}$	16	+	$p=1$	ND	87JOR/BEN
XJ1	$\{x_{ij}, T_{ij}, \ln p(O_2)_i\}$	7	+	$p=0.2$	ND	87JOR/BEN
XJ3	$\{x_{ij}, T_{ij}, \ln p(O_2)_i\}$	7	+	$p=0.02$	ND	87JOR/BEN
XI1	$\{x_{ij}, T_{ij}, \ln p(O_2)_i\}$	9	+	$p=0.2$	XRD	88IKE/NAG
ZJ0	$\{z_{ij}, T_{ij}, \ln p(O_2)_i\}$	17	−	$p=1$	ND	87JOR/BEN
ZJ1	$\{z_{ij}, T_{ij}, \ln p(O_2)_i\}$	7	−	$p=0.2$	ND	87JOR/BEN
ZJ3	$\{z_{ij}, T_{ij}, \ln p(O_2)_i\}$	7	−	$p=0.02$	ND	87JOR/BEN
ZI1	$\{z_{ij}, T_{ij}, \ln p(O_2)_i\}$	10	−	$p=0.2$	TGA	88IKE/NAG
Zt0	$\{z_{ij}, T_{ij}, \ln p(O_2)_i\}$	7	−	$p=1$	TGA	87STR/CAP
Zt1	$\{z_{ij}, T_{ij}, \ln p(O_2)_i\}$	7	−	$p=0.25$	TGA	87STR/CAP
Zt3	$\{z_{ij}, T_{ij}, \ln p(O_2)_i\}$	7	−	$p=0.050$	TGA	87STR/CAP
Zt4	$\{z_{ij}, T_{ij}, \ln p(O_2)_i\}$	7	−	$p=0.01$	TGA	87STR/CAP
Zt6	$\{z_{ij}, T_{ij}, \ln p(O_2)_i\}$	4	−	$p=0.001$	TGA	87STR/CAP
ZS0	$\{z_{ij}, T_{ij}, \ln p(O_2)_i\}$	35	−	$p=0.74$	TGA	88SPE/SPA
ZS1	$\{z_{ij}, T_{ij}, \ln p(O_2)_i\}$	8	−	$p=0.36$	TGA	88SPE/SPA
ZT0	$\{z_{ij}, T_{ij}, \ln p(O_2)_i\}$	8	−	$p=1$	TGA	88TOU/MAR
ZT1	$\{z_{ij}, T_{ij}, \ln p(O_2)_i\}$	6	−	$p=0.2$	TGA	88TOU/MAR
ZY0	$\{z_{ij}, T_{ij}, \ln p(O_2)_i\}$	26	−	$p=1$	TGA	88YAM/TER
ZY0a	$\{z_{ij}, T_{ij}, \ln p(O_2)_i\}$	9	−	$p=0.7$	TGA	88YAM/TER
ZY1	$\{z_{ij}, T_{ij}, \ln p(O_2)_i\}$	9	−	$p=0.4$	TGA	88YAM/TER
ZY1a	$\{z_{ij}, T_{ij}, \ln p(O_2)_i\}$	29	−	$p=0.2$	TGA	88YAM/TER
ZY3	$\{z_{ij}, T_{ij}, \ln p(O_2)_i\}$	24	−	$p=0.053$	TGA	88YAM/TER
ZY4	$\{z_{ij}, T_{ij}, \ln p(O_2)_i\}$	26	−	$p=0.013$	TGA	88YAM/TER
ZY5	$\{z_{ij}, T_{ij}, \ln p(O_2)_i\}$	24	−	$p=0.005$	TGA	88YAM/TER
ZY6	$\{z_{ij}, T_{ij}, \ln p(O_2)_i\}$	9	−	$p=0.0022$	TGA	88YAM/TER
ZY7	$\{z_{ij}, T_{ij}, \ln p(O_2)_i\}$	6	−	$p=3\cdot10^{-4}$	TGA	88YAM/TER
ZB8	$\{z_{ij}, T_{ij}, \ln p(O_2)_i\}$	10	−	$p=1.3\cdot10^{-4}$	TGA	89BRY/GAL
ZBA	$\{z_{ij}, T_{ij}, \ln p(O_2)_i\}$	4	−	$p=1.8\cdot10^{-5}$	TGA	89BRY/GAL
ZF0	$\{z_{ij}, T_{ij}, \ln p(O_2)_i\}$	12	−	$p = 1$	TGA	90FUE/IDE
ZF1	$\{z_{ij}, T_{ij}, \ln p(O_2)_i\}$	12	−	$p = 0.4$	TGA	90FUE/IDE
ZF2	$\{z_{ij}, T_{ij}, \ln p(O_2)_i\}$	11	−	$p = 0.1$	TGA	90FUE/IDE
ZF3	$\{z_{ij}, T_{ij}, \ln p(O_2)_i\}$	10	−	$p = 0.05$	TGA	90FUE/IDE
ZF4	$\{z_{ij}, T_{ij}, \ln p(O_2)_i\}$	9	−	$p = 0.007$	TGA	90FUE/IDE
ZK0	$\{z_{ij}, T_{ij}, \ln p(O_2)_i\}$	12	−	$p = 1$	TGA	94KIM/GAS
ZK2	$\{z_{ij}, T_{ij}, \ln p(O_2)_i\}$	12	−	$p = 0.1$	TGA	94KIM/GAS
ZK4	$\{z_{ij}, T_{ij}, \ln p(O_2)_i\}$	11	−	$p = 0.01$	TGA	94KIM/GAS
ZK6	$\{z_{ij}, T_{ij}, \ln p(O_2)_i\}$	10	−	$p = 0.001$	TGA	94KIM/GAS
ZK8	$\{z_{ij}, T_{ij}, \ln p(O_2)_i\}$	8	−	$p = 1\cdot10^{-4}$	TGA	94KIM/GAS
ZKA	$\{z_{ij}, T_{ij}, \ln p(O_2)_i\}$	8	−	$p = 1\cdot10^{-5}$	TGA	94KIM/GAS
ZKC	$\{z_{ij}, T_{ij}, \ln p(O_2)_i\}$	3	−	$p = 1\cdot10^{-6}$	TGA	94KIM/GAS

TABLE 2. Experimental results available for the assessment of the $YBa_2Cu_3O_{6+z}$ phase thermodynamics—Continued

Code	Set of values	N_i	Inc.	v_i	Method	Reference
ZL0	$\{z_{ij}, T_{ij}, \ln p(O_2)_i\}$	25	+	$p = 1$	TGA	89LIN/HUN
ZL2	$\{z_{ij}, T_{ij}, \ln p(O_2)_i\}$	12	+	$p = 0.1$	TGA	89LIN/HUN
ZL4	$\{z_{ij}, T_{ij}, \ln p(O_2)_i\}$	11	+	$p = 0.01$	TGA	89LIN/HUN
ZL6	$\{z_{ij}, T_{ij}, \ln p(O_2)_i\}$	9	+	$p = 0.001$	TGA	89LIN/HUN
ZL8	$\{z_{ij}, T_{ij}, \ln p(O_2)_i\}$	6	+	$p = 1 \cdot 10^{-4}$	TGA	89LIN/HUN
ZLA	$\{z_{ij}, T_{ij}, \ln p(O_2)_i\}$	2	+	$p = 1 \cdot 10^{-5}$	TGA	89LIN/HUN
ZV0	$\{z_{ij}, T_{ij}, \ln p(O_2)_i\}$	7	+	$p = 0.89$	Analysis	89VER/BRU
ZC0	$\{z_{ij}, T_{ij}, \ln p(O_2)_i\}$	16	+	$p = 1$	TGA	92CON/KAR
ZC0a	$\{z_{ij}, T_{ij}, \ln p(O_2)_i\}$	13	+	$p = 1$	TGA	92CON/KAR
ZC2	$\{z_{ij}, T_{ij}, \ln p(O_2)_i\}$	10	+	$p = 0.09$	TGA	92CON/KAR
ZC4	$\{z_{ij}, T_{ij}, \ln p(O_2)_i\}$	7	+	$p = 0.01$	TGA	92CON/KAR
ZC6	$\{z_{ij}, T_{ij}, \ln p(O_2)_i\}$	6	+	$p = 0.0017$	TGA	92CON/KAR
ZCK	$\{z_{ij}, T_{ij}, \ln p(O_2)_i\}$	13	+	$p = 4$	TGA	92CON/KAR
ZCL	$\{z_{ij}, T_{ij}, \ln p(O_2)_i\}$	11	+	$p = 11$	TGA	92CON/KAR
ZCM	$\{z_{ij}, T_{ij}, \ln p(O_2)_i\}$	9	+	$p = 50$	TGA	92CON/KAR
Os9	$\{\ln p(O_2)_{ij}, z_{ij}, T_i\}$	22	−	$T = 838$ K	VA	87SAL/KOE
OsB	$\{\ln p(O_2)_{ij}, z_{ij}, T_i\}$	23	−	$T = 884$ K	VA	87SAL/KOE
OsD	$\{\ln p(O_2)_{ij}, z_{ij}, T_i\}$	21	−	$T = 926$ K	VA	87SAL/KOE
OsG	$\{\ln p(O_2)_{ij}, z_{ij}, T_i\}$	18	−	$T = 990$ K	VA	87SAL/KOE
OsJ	$\{\ln p(O_2)_{ij}, z_{ij}, T_i\}$	11	−	$T = 1081$ K	VA	87SAL/KOE
OBD	$\{\ln p(O_2)_{ij}, z_{ij}, T_i\}$	5	−	$T = 913$ K	emf	89BOR/NOL
OBG	$\{\ln p(O_2)_{ij}, z_{ij}, T_i\}$	4	−	$T = 993$ K	emf	89BOR/NOL
OBH	$\{\ln p(O_2)_{ij}, z_{ij}, T_i\}$	4	−	$T = 1023$ K	emf	89BOR/NOL
OK1	$\{\ln p(O_2)_{ij}, z_{ij}, T_i\}$	4	−	$T = 623$ K	TGA	87KIS/SHI
OK3	$\{\ln p(O_2)_{ij}, z_{ij}, T_i\}$	4	−	$T = 673$ K	TGA	87KIS/SHI
OK5	$\{\ln p(O_2)_{ij}, z_{ij}, T_i\}$	7	−	$T = 723$ K	TGA	87KIS/SHI
OK7	$\{\ln p(O_2)_{ij}, z_{ij}, T_i\}$	11	−	$T = 773$ K	TGA	87KIS/SHI
OK9	$\{\ln p(O_2)_{ij}, z_{ij}, T_i\}$	12	−	$T = 823$ K	TGA	87KIS/SHI
OKB	$\{\ln p(O_2)_{ij}, z_{ij}, T_i\}$	11	−	$T = 873$ K	TGA	87KIS/SHI
OKD	$\{\ln p(O_2)_{ij}, z_{ij}, T_i\}$	12	−	$T = 923$ K	TGA	87KIS/SHI
OKF	$\{\ln p(O_2)_{ij}, z_{ij}, T_i\}$	10	−	$T = 973$ K	TGA	87KIS/SHI
OKH	$\{\ln p(O_2)_{ij}, z_{ij}, T_i\}$	10	−	$T = 1023$ K	TGA	87KIS/SHI
OKJ	$\{\ln p(O_2)_{ij}, z_{ij}, T_i\}$	9	−	$T = 1073$ K	TGA	87KIS/SHI
OKL	$\{\ln p(O_2)_{ij}, z_{ij}, T_i\}$	9	−	$T = 1123$ K	TGA	87KIS/SHI
OKN	$\{\ln p(O_2)_{ij}, z_{ij}, T_i\}$	7	−	$T = 1173$ K	TGA	87KIS/SHI
OKQ	$\{\ln p(O_2)_{ij}, z_{ij}, T_i\}$	7	−	$T = 1223$ K	TGA	87KIS/SHI
OKS	$\{\ln p(O_2)_{ij}, z_{ij}, T_i\}$	4	−	$T = 1273$ K	TGA	87KIS/SHI
OT7	$\{\ln p(O_2)_{ij}, z_{ij}, T_i\}$	5	−	$T = 773$ K	TGA	88TOU/MAR
OTB	$\{\ln p(O_2)_{ij}, z_{ij}, T_i\}$	4	−	$T = 873$ K	TGA	88TOU/MAR
OTJ	$\{\ln p(O_2)_{ij}, z_{ij}, T_i\}$	3	−	$T = 1073$ K	TGA	88TOU/MAR
OS7	$\{\ln p(O_2)_{ij}, z_{ij}, T_i\}$	10	−	$T = 776$ K	TGA	88SPE/SPA
OSB	$\{\ln p(O_2)_{ij}, z_{ij}, T_i\}$	10	−	$T = 861$ K	TGA	88SPE/SPA
OSD	$\{\ln p(O_2)_{ij}, z_{ij}, T_i\}$	10	−	$T = 938$ K	TGA	88SPE/SPA
OSH	$\{\ln p(O_2)_{ij}, z_{ij}, T_i\}$	10	−	$T = 1012$ K	TGA	88SPE/SPA
OSJ	$\{\ln p(O_2)_{ij}, z_{ij}, T_i\}$	10	−	$T = 1070$ K	TGA	88SPE/SPA
OSM	$\{\ln p(O_2)_{ij}, z_{ij}, T_i\}$	10	−	$T = 1148$ K	TGA	88SPE/SPA
OM3	$\{\ln p(O_2)_{ij}, z_{ij}, T_i\}$	19	−	$T = 673$ K	VA	89MEU/NAE
OM4	$\{\ln p(O_2)_{ij}, z_{ij}, T_i\}$	20	−	$T = 698$ K	VA	89MEU/NAE
OM5	$\{\ln p(O_2)_{ij}, z_{ij}, T_i\}$	22	−	$T = 723$ K	VA	89MEU/NAE
OM6	$\{\ln p(O_2)_{ij}, z_{ij}, T_i\}$	20	−	$T = 748$ K	VA	89MEU/NAE
OM7	$\{\ln p(O_2)_{ij}, z_{ij}, T_i\}$	26	−	$T = 773$ K	VA	89MEU/NAE
OM8	$\{\ln p(O_2)_{ij}, z_{ij}, T_i\}$	25	−	$T = 798$ K	VA	89MEU/NAE
OM9	$\{\ln p(O_2)_{ij}, z_{ij}, T_i\}$	26	−	$T = 823$ K	VA	89MEU/NAE
OMA	$\{\ln p(O_2)_{ij}, z_{ij}, T_i\}$	28	−	$T = 848$ K	VA	89MEU/NAE
OMB	$\{\ln p(O_2)_{ij}, z_{ij}, T_i\}$	28	−	$T = 873$ K	VA	89MEU/NAE
OMC	$\{\ln p(O_2)_{ij}, z_{ij}, T_i\}$	30	−	$T = 898$ K	VA	89MEU/NAE
OMD	$\{\ln p(O_2)_{ij}, z_{ij}, T_i\}$	30	−	$T = 923$ K	VA	89MEU/NAE
OME	$\{\ln p(O_2)_{ij}, z_{ij}, T_i\}$	31	−	$T = 948$ K	VA	89MEU/NAE
OMF	$\{\ln p(O_2)_{ij}, z_{ij}, T_i\}$	32	−	$T = 973$ K	VA	89MEU/NAE
OMG	$\{\ln p(O_2)_{ij}, z_{ij}, T_i\}$	32	−	$T = 998$ K	VA	89MEU/NAE
OMH	$\{\ln p(O_2)_{ij}, z_{ij}, T_i\}$	30	−	$T = 1023$ K	VA	89MEU/NAE
Ot3	$\{\ln p(O_2)_{ij}, z_{ij}, T_i\}$	26	−	$T = 673$ K	emf	89TET/TAN

TABLE 2. Experimental results available for the assessment of the $YBa_2Cu_3O_{6+z}$ phase thermodynamics—Continued

Code	Set of values	N_i	Inc.	v_i	Method	Reference
Ot4	$\{\ln p(O_2)_{ij}, z_{ij}, T_i\}$	27	−	$T=698$ K	emf	89TET/TAN
Ot5	$\{\ln p(O_2)_{ij}, z_{ij}, T_i\}$	27	−	$T=723$ K	emf	89TET/TAN
Ot6	$\{\ln p(O_2)_{ij}, z_{ij}, T_i\}$	28	−	$T=748$ K	emf	89TET/TAN
Ot7	$\{\ln p(O_2)_{ij}, z_{ij}, T_i\}$	29	−	$T=773$ K	emf	89TET/TAN
Ot9	$\{\ln p(O_2)_{ij}, z_{ij}, T_i\}$	28	−	$T=823$ K	emf	89TET/TAN
OtB	$\{\ln p(O_2)_{ij}, z_{ij}, T_i\}$	24	−	$T=873$ K	emf	89TET/TAN
OGB	$\{\ln p(O_2)_{ij}, z_{ij}, T_i\}$	38	+	$T=873$ K	TGA	89GER/PIC
Oc5	$\{\ln p(O_2)_{ij}, z_{ij}, T_i\}$	28	+	$T=723$ K	VA	91SCH/HAR
Oc6	$\{\ln p(O_2)_{ij}, z_{ij}, T_i\}$	36	+	$T=748$ K	VA	91SCH/HAR
Oc7	$\{\ln p(O_2)_{ij}, z_{ij}, T_i\}$	33	+	$T=773$ K	VA	91SCH/HAR
Oc9	$\{\ln p(O_2)_{ij}, z_{ij}, T_i\}$	32	+	$T=823$ K	VA	91SCH/HAR
OcB	$\{\ln p(O_2)_{ij}, z_{ij}, T_i\}$	30	+	$T=873$ K	VA	91SCH/HAR
OcD	$\{\ln p(O_2)_{ij}, z_{ij}, T_i\}$	28	+	$T=923$ K	VA	91SCH/HAR
Om7	$\{\ln p(O_2)_{ij}, z_{ij}, T_i\}$	19	+	$T=773$ K	emf	92MAT/JAC
OmB	$\{\ln p(O_2)_{ij}, z_{ij}, T_i\}$	18	+	$T=873$ K	emf	92MAT/JAC
OmF	$\{\ln p(O_2)_{ij}, z_{ij}, T_i\}$	12	+	$T=973$ K	emf	92MAT/JAC
OmJ	$\{\ln p(O_2)_{ij}, z_{ij}, T_i\}$	8	+	$T=1073$ K	emf	92MAT/JAC
OmN	$\{\ln p(O_2)_{ij}, z_{ij}, T_i\}$	6	+	$T=1173$ K	emf	92MAT/JAC
OmQ	$\{\ln p(O_2)_{ij}, z_{ij}, T_i\}$	6	+	$T=1273$ K	emf	92MAT/JAC
N1	$\{\ln p(O_2)_{ij}, T_{ij}, z_i\}$	55	−	$z=0.978$	VA	89VER/BRU
N2	$\{\ln p(O_2)_{ij}, T_{ij}, z_i\}$	55	+	$z=0.922$	VA	89VER/BRU
N3	$\{\ln p(O_2)_{ij}, T_{ij}, z_i\}$	44	+	$z=0.801$	VA	89VER/BRU
N4	$\{\ln p(O_2)_{ij}, T_{ij}, z_i\}$	77	+	$z=0.632$	VA	89VER/BRU
N5	$\{\ln p(O_2)_{ij}, T_{ij}, z_i\}$	66	+	$z=0.508$	VA	89VER/BRU
N6	$\{\ln p(O_2)_{ij}, T_{ij}, z_i\}$	55	+	$z=0.404$	VA	89VER/BRU
N7	$\{\ln p(O_2)_{ij}, T_{ij}, z_i\}$	22	+	$z=0.285$	VA	89VER/BRU
VT1	$\{\ln p(O_2)_{ij}, T_{ij}, V_i\}^d$	86	−	n/a	VA	94TAR/GUS
VT2	$\{\ln p(O_2)_{ij}, T_{ij}, V_i\}^d$	41	−	n/a	VA	94TAR/GUS
VT3	$\{\ln p(O_2)_{ij}, T_{ij}, V_i\}^d$	39	−	n/a	VA	94TAR/GUS
VT4	$\{\ln p(O_2)_{ij}, T_{ij}, V_i\}^d$	28	−	n/a	VA	94TAR/GUS
VT5	$\{\ln p(O_2)_{ij}, T_{ij}, V_i\}^d$	41	−	n/a	VA	94TAR/GUS
VT6	$\{\ln p(O_2)_{ij}, T_{ij}, V_i\}^d$	51	−	n/a	VA	94TAR/GUS
VT7	$\{\ln p(O_2)_{ij}, T_{ij}, V_i\}^d$	35	−	n/a	VA	94TAR/GUS
VT8	$\{\ln p(O_2)_{ij}, T_{ij}, V_i\}^d$	50	−	n/a	VA	94TAR/GUS
VT9	$\{\ln p(O_2)_{ij}, T_{ij}, V_i\}^d$	29	−	n/a	VA	94TAR/GUS
VTA	$\{\ln p(O_2)_{ij}, T_{ij}, V_i\}^d$	30	−	n/a	VA	94TAR/GUS
VTB	$\{\ln p(O_2)_{ij}, T_{ij}, V_i\}^d$	31	−	n/a	VA	94TAR/GUS
VTC	$\{\ln p(O_2)_{ij}, T_{ij}, V_i\}^d$	40	−	n/a	VA	94TAR/GUS
VTD	$\{\ln p(O_2)_{ij}, T_{ij}, V_i\}^d$	47	−	n/a	VA	94TAR/GUS
VTE	$\{\ln p(O_2)_{ij}, T_{ij}, V_i\}^d$	43	−	n/a	VA	94TAR/GUS
VTF	$\{\ln p(O_2)_{ij}, T_{ij}, V_i\}^d$	43	−	n/a	VA	94TAR/GUS
VTG	$\{\ln p(O_2)_{ij}, T_{ij}, V_i\}^d$	47	−	n/a	VA	94TAR/GUS
PG	$\{\Delta_{ox}H'_{O_2,ij}, z_{ij}, T_i\}$	19	−	$T=873$ K	Calorimetry	89GER/PIC
PP1	$\{\Delta H_{ij}, z'_{ij}, T'_i\}^e$	10	+	n/a	Calorimetry	89PAR/NAV
PP2	$\{\Delta H_{ij}, z'_{ij}, T'_i\}^e$	14	+	n/a	Calorimetry	89PAR/NAV
PP3	$\{\Delta H_{ij}, z'_{ij}, T'_i\}^e$	3	+	n/a	Calorimetry	89PAR/NAV
S	$\{S_{ij}, z_{ij}, T_i\}$	6	+	$T=298$ K	AC	
CG7	$\{C_{p,ij}, T_{ij}, z_i\}$	7	+	$z=0.70$	AC	88GAV/GOR
CG9	$\{C_{p,ij}, T_{ij}, z_i\}$	7	+	$z=0.85$	AC	88GAV/GOR
CJ9	$\{C_{p,ij}, T_{ij}, z_i\}$	5	+	$z=0.9$	AC	89JUN/ECK
CS9	$\{C_{p,ij}, T_{ij}, z_i\}$	9	+	$z=0.9$	AC	90SHA/WES

TABLE 2. Experimental results available for the assessment of the $YBa_2Cu_3O_{6+z}$ phase thermodynamics—Continued

Code	Set of values	N_i	Inc.	v_i	Method	Reference
CAA	$\{C_{pz,ij}, T_{ij}, z_i\}$	7	+	$z=0.96$	AC	91ATA/HON
CA	$\{C_{pz,ij}, T_{ij}, z_i\}$	2	−	$z=1.0$	AC	88SHE/CHU
CM4	$\{C_{pz,ij}, T_{ij}, z_i\}$	9	−	$z=0.4$	DSC	90MAT/FUJ
CM7	$\{C_{pz,ij}, T_{ij}, z_i\}$	11	−	$z=0.65$	DSC	90MAT/FUJ
CM8	$\{C_{pz,ij}, T_{ij}, z_i\}$	10	−	$z=0.82$	DSC	90MAT/FUJ
CA5	$\{C_{pz,ij}, T_{ij}, z_i\}$	21	−	$z=0.5$	DSC	91SHA/OZE
CA9	$\{C_{pz,ij}, T_{ij}, z_i\}$	20	−	$z=0.85$	DSC	91SHA/OZE
HG	$\{\Delta_{ox}H_{ij}, z_{ij}, T_i\}$		−	$T=298$ K	Calorimetry	89GRU/PIV
HE	$\{\Delta_{ox}H_{ij}, z_{ij}, T_i\}$		−	$T=298$ K	Calorimetry	91GAR/RAI
HC	$\{\Delta_{ox}H_{ij}, z_{ij}, T_i\}$		−	$T=298$ K	Calorimetry	92CHO/KAN
HI	$\{\Delta_{ox}H_{ij}, z_{ij}, T_i\}$		−	$T=298$ K	Calorimetry	92IDE/TAK
HP	$\{\Delta_{ox}H_{ij}, z_{ij}, T_i\}$		−	$T=298$ K	Calorimetry	93PRI/ZIN
HM	$\{\Delta_{ox}H_{ij}, z_{ij}, T_i\}$	4	+	$T=298$ K	Calorimetry	88MOR/SON
Hm	$\{\Delta_{ox}H_{ij}, z_{ij}, T_i\}$	2	+	$T=298$ K	Calorimetry	95MON/POP
Ha	$\{\Delta_{ox}H_{ij}, z_{ij}, T_i\}$	5	+	$T=298$ K	Calorimetry	93MAT/POP
HZ	$\{\Delta_{ox}H_{ij}, z_{ij}, T_i\}$	7	+	$T=298$ K	Calorimetry	92ZHO/NAV
HH	$\{\Delta_{ox}H_{ij}, z_{ij}, T_i\}$		+	$T=298$ K	Calorimetry	95HEN/ZHE
GA	$\{\Delta_{ox}G_{ij}, T_{ij}, \ln p(O_2)_i\}$		−	$p=1$	emf	90AZA/SRE
GF	$\{\Delta_{ox}G_{ij}, T_{ij}, \ln p(O_2)_i\}$		−	$p=0.21$	emf	90FAN/II
GS	$\{\Delta_{ox}G_{ij}, T_{ij}, \ln p(O_2)_i\}$	26	+	$p=1$	emf	91SKO/PAS

Plus means that the experiment is included into the final assessment, minus means that it is not (see also Table 3).

"a" means not applicable, p in this column means dimentionless quantity p/p^o, where $p^o=101\ 325$ Pa.

XRD—X-ray diffraction, resistivity—measurements of the sample resistance, TGA—thermal gravimetry analysis, ND—neutron diffraction, analysis—chemical analysis of the composition, VA—volumetric analysis, emf—electromotive force, AC—adiabatic calorimetry, DSC—differential scanning calorimetry.

The experimental point looks like $\{\ln p(O_2)_{ij}, T_{ij}, V_i, z_i^o, m_i^o\}$.

The experimental point looks like $\{\Delta H_{ij}, z'_{ij}, T'_i, z''_i, T''_i\}$.

The references for set S are 88GAV/GOR, 89JUN/ECK, 90SHA/WES, 91ATA/HON, 88SHE/CHU.

experiment. Everywhere where it was possible, we have preferred employing direct experimental results in order not to introduce additional errors during preprocessing. A code was assigned to each experiment (see Table 2) and all the data displays are referred to this code. For convenience, in this section these codes are listed after references in parentheses.

Then the relationship between the measured property and the controlled variables can be discussed. In the general form the relationship can be expressed as

$$y_{ij}=y_{ij}^{calc}\{u_{ij}, v_i; \Theta\}+\varepsilon_{ij}. \tag{23}$$

where y^{calc} is the value that is calculated by thermodynamic laws at given u_{ij} and v_i and differs from the experimentally measured y_{ij} by the experimental error ε_{ij}. The discussion of errors will be delayed until Sec. 4. Θ is the vector of unknown parameters to be determined. As was discussed in the previous section, all the thermodynamic properties of the $YBa_2Cu_3O_{6+z}$ phase, y_{ij}^{calc}, can be obtained from Eq. (2) by means of algebraic and/or numerical methods. This means that vector Θ contains the same set of unknown parameters for all the equations described below. Note that some parameters may vanish during differentiation of Eq. (2).

The results of the experiments in each category can be compared with each other directly. The results of this comparison and the quality of experiments are discussed below and the further partition of the experiments in each group into smaller sets of about the same quality is presented. Comparison among different experimental groups is impossible without simultaneous assessment, as will be discussed in Secs. 4 and 5.

Figures with the experimental points are given for most experiments. In the figures, there are also three solutions: two of them are obtained in the present work (ML and WLS) and one is taken from the previous assessment by 93VOR/DEG. Figure 23 is exception from this rule and is discussed separately. The solutions are discussed later in Secs. 4 to 6.

Table 2 summarizes all the experimental information available. The table contains the codes assigned to the experiments, references, and information on experiments: the number of experimental points, whether the experiment was included in the assessment (column *inc*) and the value of v_i. The different experimental groups are separated by solid lines and subgroups of about the same quality are separated by dashed lines. The division into the experimental groups is summed up in Table 3.

TABLE 3. Grouping the experiments

Quantity[a]	Group	Codes of the experiments	Inc.[b]
Temperature of T-O phase transition	T_O	TB1, TE, TF, TK, TT, TY, To, Tp, Tu, TW, TB2	+[c]
Temperature of T-O phase transition	T_z	TM1, TM2	−
Oxygen occupancies	X	XJ0, XJ1, XJ3, XI1	+
Index z	Z_b	ZJ0, ZJ1, ZJ3, ZI1	−
Index z	Z_g	Zt0, Zt1, Zt3, Zt4, Zt6, ZS0, ZS1, ZT0, ZT1, ZY0, ZY0a, ZY1, ZY1a, ZY3, ZY4, ZY5, ZY6, ZY7, ZB8, ZBA, ZF0, ZF1, ZF2, ZF3, ZF4, ZK0, ZK2, ZK4, ZK6, ZK8, ZKA, ZKC	−
Index z	Z	ZL0, ZL2, ZL4, ZL6, ZL8, ZLA, ZV0, ZC0, ZC0a, ZC2, ZC4, ZC6, ZCK, ZCL, ZCM	+
Oxygen partial pressure (T=const)	O_b	Os9, OsB, OsD, OsG, OsJ, OBD, OBG, OBH, OK1, OK3, OK5, OK7	−
Oxygen partial pressure (T=const)	O_g	OK9, OKB, OKD, OKF, OKH, OKJ, OKL, OKN, OKQ, OKS, OT7, OTB, OTJ, OS7, OSB, OSD, OSH, OSJ, OSM, OM3, OM4, OM5, OM6, OM7, OM8, OM9, OMA, OMB, OMC, OMD, OME, OMF, OMG, OMH, Ot3, Ot4, Ot5, Ot6, Ot7, Ot9, OtB	−
Oxygen partial pressure (T=const)	O	OGB, Oc5, Oc6, Oc7, Oc9, OcB, OcD, Om7, OmB, OmF, OmJ, OmN, OmQ	+
Oxygen partial pressure (z=const)	N	N2, N3, N4, N5, N6, N7	+[d]
Oxygen partial pressure (V=const)	V	VT1, VT2, VT3, VT4, VT5, VT6, VT7, VT8, VT9, VTA, VTB, VTC, VTD, VTE, VTF, VTG	−
Partial enthalpy	P_b	PG	−
Drop enthalpy	P	PP1, PP2, PP3	+
Entropy	S	S	+
Heat capacity	C	CG7, CG9, CJ9, CS9, CAA, CsA	+
Heat capacity	C_h	CM4, CM7, CM8, Ca5, Ca9	−
Enthalpy	H_b	HG, Hg, HC, HI, HP	−
Enthalpy	H	HM, Hm, Ha, HZ, HH	+
Gibbs energy	G_b	GA, GF	−
Gibbs energy	G	GS	+

[a]See Sec. 3 and Table 2 for explanations what the quantity means, T-O is Tetragonal-orthorhombic.
[b]Plus means that the group is included into the final assessment, minus means that it is not (see also Table 2). Explanations are in Sec. 4.2.
[c]Ts was excluded because it was assumed to be the outlier.
[d]N1 was excluded because it was assumed to be the outlier.

3.1. Tetragonal-Orthorhombic Phase Transition and Oxygen Occupancies

It appears that the first measurements related to thermodynamic properties of the $YBa_2Cu_3O_{6+z}$ phase were the determination of temperatures of the tetragonal-orthorhombic phase transition. In a typical experiment the sample of the $YBa_2Cu_3O_{6+z}$ phase was heated or cooled in a controlled atmosphere with known oxygen partial pressure. The phase transition was detected by the bend in the thermogravimetry (TGA) or resistivity curve, or by x-ray methods. Then, we have a number of experimental points in the form $\{T_{ij}, \ln p(O_2)_{ij}\}$ (see Fig. 1 and Table 2). One can compute the temperature of the phase transition T_{ij}^{calc} at a given oxygen partial pressure by solving the system of two equations (7) and (8) for the two unknowns z and T, assuming that x is equal to zero.

The experiments carried out by 88MEU/RUP (TM1) and 89MEU/NAE (TM2) were quite similar except that the oxygen partial pressure was not fixed during the heating/cooling cycle. One problem is that the authors have presented not the original experimental values in the form $\{T_{ij}, \ln p(O_2)_{ij}\}$ but rather recalculated $p(O_2)_{ij}$ to the index z_{ij} according to their own measurements. Thus, here we have the experimental points in the form $\{T_{ij}, z_{ij}\}$ (Table 2 and Fig. 2). The calculation of T_{ij}^{calc} at the given z_{ij} is easier than in the previous case. It is necessary to solve one equation (7) for one unknown T. In the simplest case the solution is even possible in closed form. However, it should be particularly mentioned that in this case we don't have the results of the original experiments, and it is very difficult to estimate uncertainties in the values of z_{ij} ascribed by the authors to the measured values of the temperature of the phase transition.

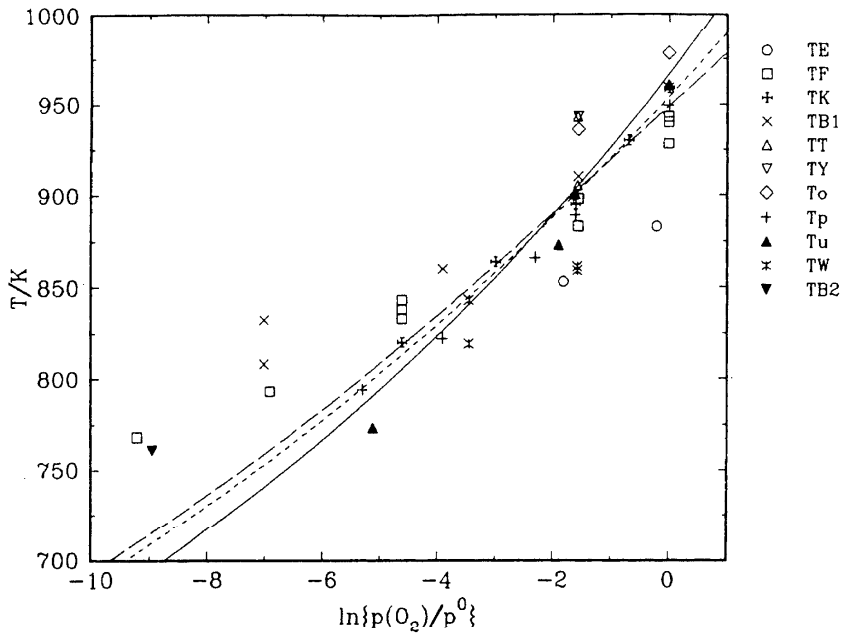

FIG. 1. The temperatures of the phase transition as a function of the oxygen partial pressure. The solid line is solution ML, the long dashed line is solution WLS, the short dashed line is the solution by 93VOR/DEG.

The oxygen occupancies in the sublattices (a) and (b) (see Eq. 1) have been measured by 87JOR/BEN (XJ0, XJ1, XJ3) and 88IKE/NAG (XI1), and Eq. (4) gives us the equilibrium value of the order parameter x. Neutron diffraction has been employed in the first work and profile fitting of x-ray diffraction reflections in the second one. The experiments were carried out at constant oxygen partial pressure and at several temperatures, and the experimental points look like $\{x_{ij}, T_{ij}, \ln p(O_2)_i\}$ (see Table 2 and Fig. 3). Computing the value of x_{ij}^{calc} at given temperature and oxygen partial pressure is done numerically by solving the system of Eqs. (5) and (8) for two unknowns, index z, and the value of the equilibrium order parameter x.

3.2. Oxygen Partial Properties

In most experiments, the relationship between the oxygen partial pressure over the $YBa_2Cu_3O_{6+z}$ phase, index z, and

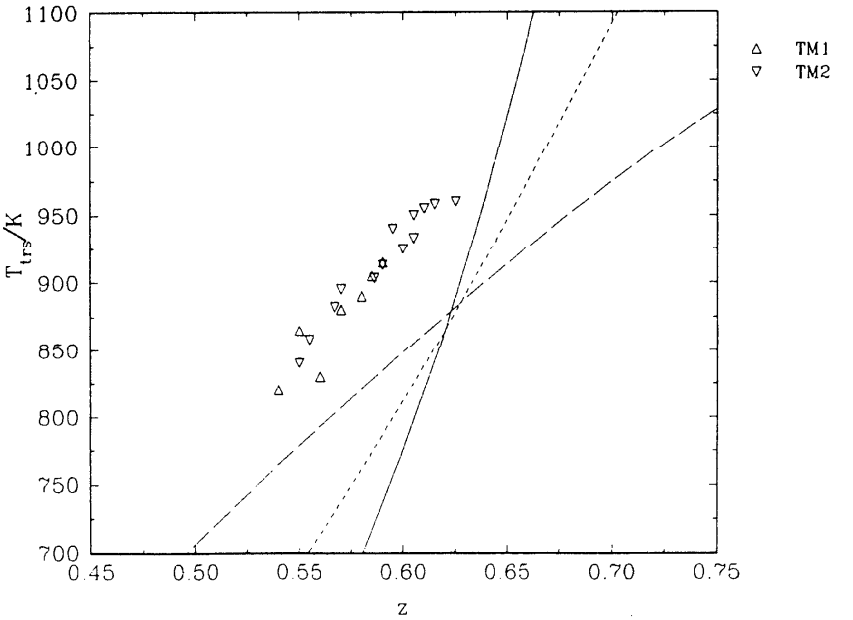

FIG. 2. The temperatures of the phase transition as a function of index z. These experimental values have not been included in the final assessment. The solid line is solution ML, the long dashed line is solution WLS, the short dashed line is the solution by 93VOR/DEG.

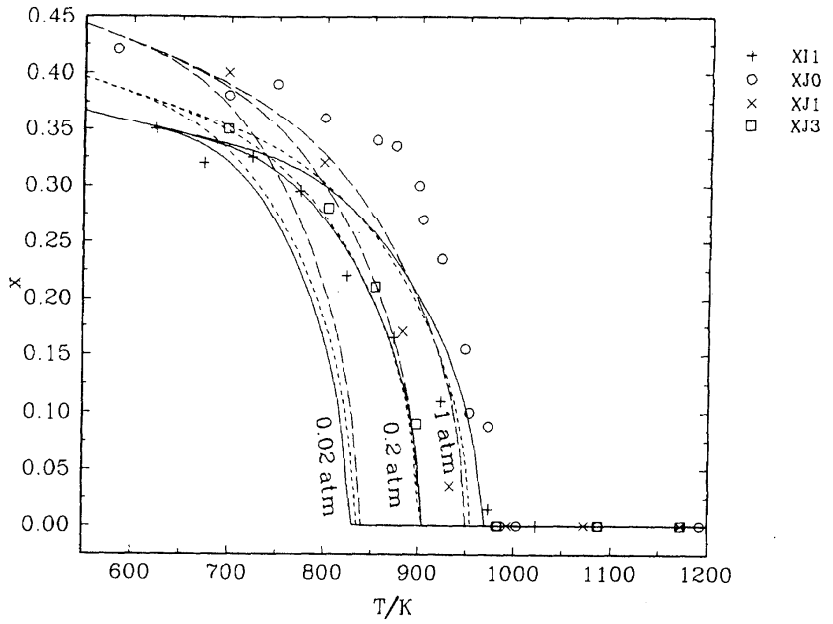

FIG. 3. The order parameter, x, as a function of the temperature at fixed oxygen partial pressures. The solid line is solution ML, the long dashed line is solution WLS, the short dashed line is the solution by 93VOR/DEG.

temperature has been studied. Because of the Gibbs phase rule, one can state that $f\{\ln p(O_2), T, z\} = 0$. There are many approaches to study this two-dimensional surface and it seems that all of them have been implemented in the case of the $YBa_2Cu_3O_{6+z}$ phase.

It is rather simple to control the oxygen partial pressure over the $YBa_2Cu_3O_{6+z}$ phase. Then, TGA allows us to measure the weight of the sample as a function of temperature and thus to measure the dependence of the index z on temperature at constant partial pressure. This gives experimental

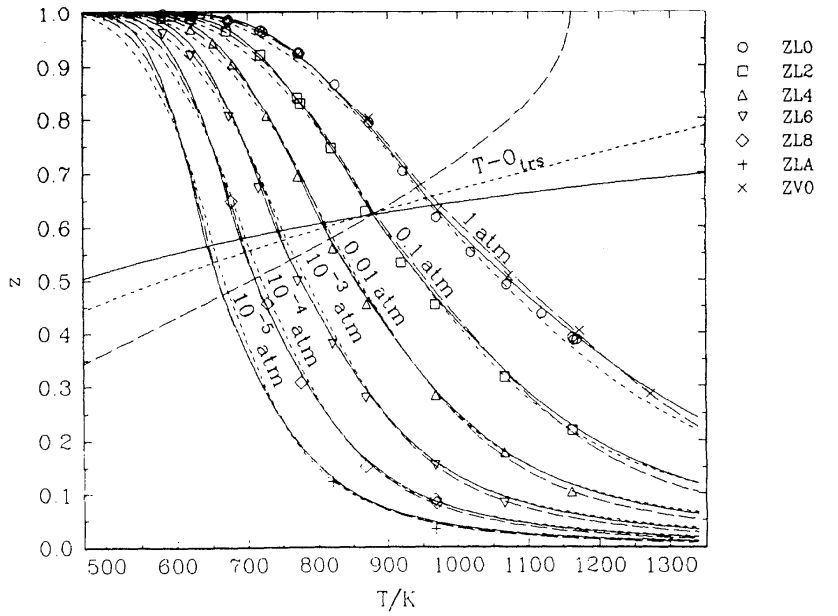

FIG. 4. Stoichiometric index z as a function of the temperature at fixed oxygen partial pressures: 89LIN/HUN and 89VER/BRU. The solid line is solution ML, the long dashed line is solution WLS, the short dashed line is the solution by 93VOR/DEG. Lines labeled T-O_{trs} show the calculated tetragonal-orthorhombic phase transition location.

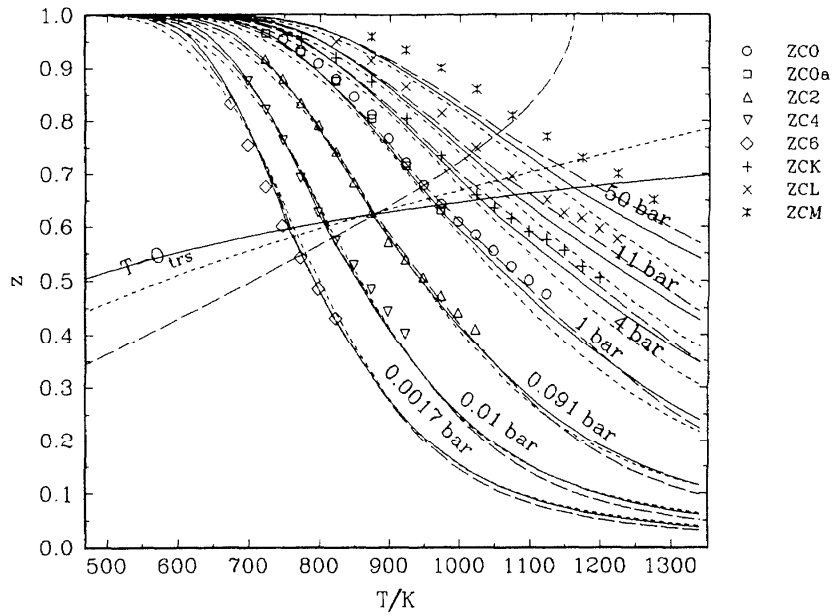

FIG. 5. Stoichiometric index z as a function of the temperature at fixed oxygen partial pressures: 92CON/KAR. The solid line is solution ML, the long dashed line is solution WLS, the short dashed line is the solution by 93VOR/DEG. Lines labeled T-O_{trs} show the calculated tetragonal-orthorhombic phase transition location.

points in the form $\{z_{ij}, T_{ij}, \ln p(O_2)_i\}$ and it is possible to calculate z_{ij}^{calc} by solving the system of Eqs. (5) and (8) for the two unknowns, index z, and the value of the equilibrium order parameter x.

All the experiments in this category were divided into three groups, Z_b, Z_g, and Z (see Table 3) based on the fact that most researchers have presented their results in graphic form. The results in group Z are available as numbers and they should be considered as most reliable. It is interesting that, if alternatively we divided the papers based on our expert opinion, neglecting whether there are numeric results or not, the same studies that are now in group Z would have been marked as the best ones. For the rest of the papers, numerical values have been obtained from figures by

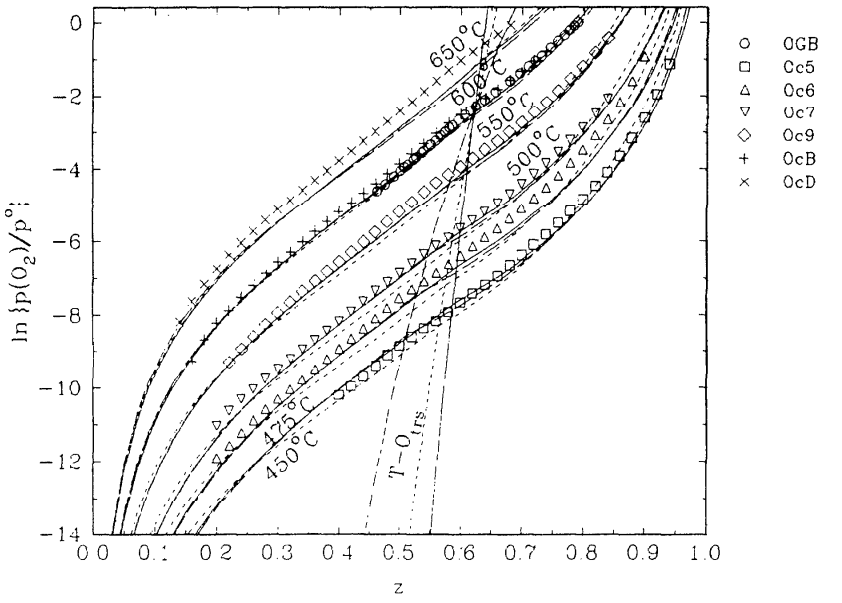

FIG. 6. The oxygen partial pressure as a function of stoichiometric index z at constant temperatures: 89GER/PIC and 91SCH/HAR. The solid line is solution ML, the long dashed line is solution WLS, the short dashed line is the solution by 93VOR/DEG. Lines labeled T-O_{trs} show the calculated tetragonal-orthorhombic phase transition location.

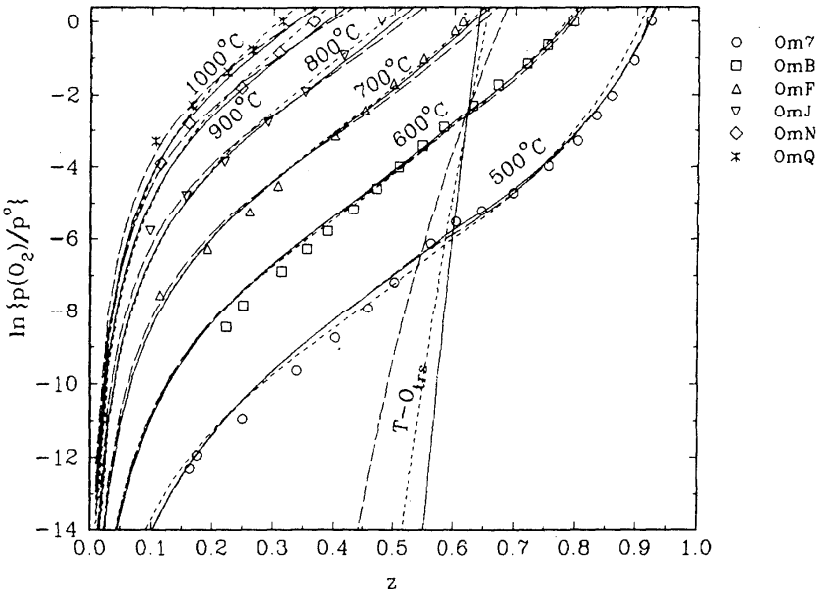

FIG. 7. The oxygen partial pressure as a function of stoichiometric index z at constant temperatures: 92MAT/JAC. The solid line is solution ML, the long dashed line is solution WLS, the short dashed line is the solution by 93VOR/DEG. Lines labeled T-O_{trs} show the calculated tetragonal-orthorhombic phase transition location.

scanning the figure and the data were put into two groups as follows. The results in group Z_g are in reasonable agreement with group Z and the results in group Z_b are not.

Figures 4 and 5 display the results of group Z: 89LIN/HUN (ZL0, ZL2, ZL4, ZL6, ZL8, ZLA), 89VER/BRU (ZV0), and 92CON/KAR (ZC0, ZC0a, ZC2, ZC6, ZCK, ZCL, ZCM).

Another approach is to study isotherms; that is, the dependence of $\ln p(O_2)$ from z at constant temperature. This approach gives experimental points in the form of

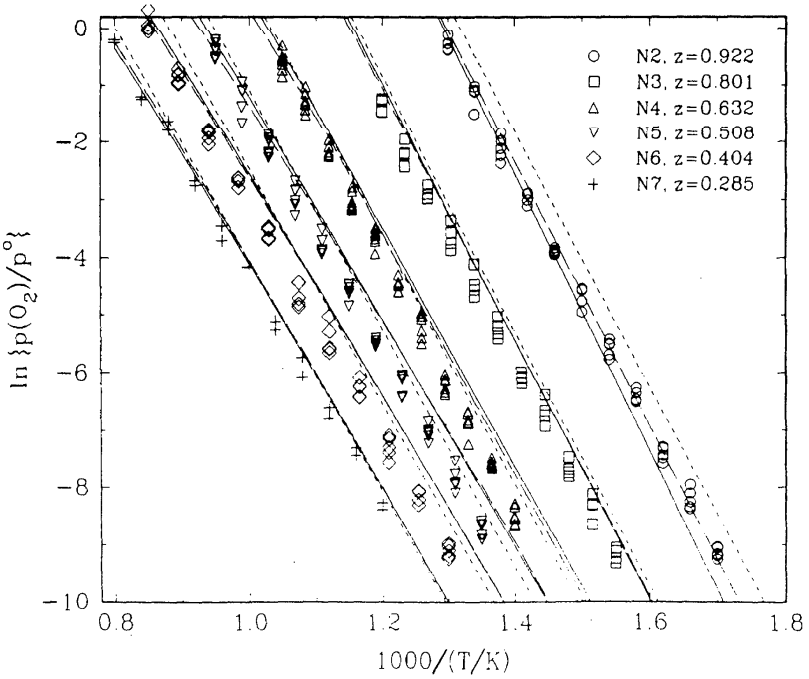

FIG. 8. The oxygen partial pressure as a function of the inverse temperature at constant z values. The solid line is solution ML, the long dashed line is solution WLS, the short dashed line is the solution by 93VOR/DEG.

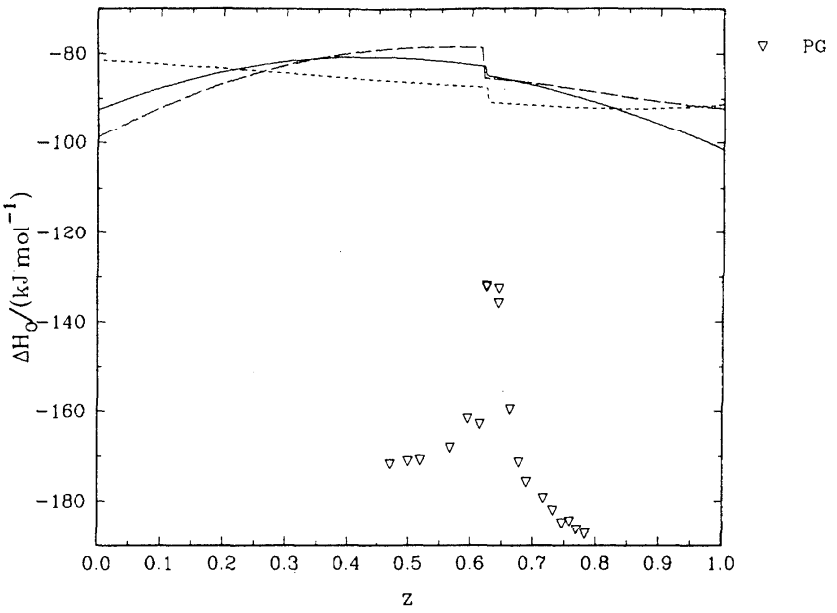

FIG. 9. The partial enthalpy as a function of stoichiometric index z at 873 K (89GER/PIC). These experimental values have not been included in the final assessment. The solid line is solution ML, the long dashed line is solution WLS, the short dashed line is the solution by 93VOR/DEG.

$\{\ln p(O_2)_{ij}, z_{ij}, T_i\}$. The techniques employed were the emf method, volumetric apparatus, and TGA (see Table 2). The work of 89MEU/NAE (OM3–OMH) is also included in this group even though the real experimental path differed from isothermal, because the results are available in the isothermal form only. It happens that computing $p(O_2)_{ij}^{\text{calc}}$ at given index z and temperature is simpler than in the previous case. Here the system of the two equations, (5) and (8) can be simplified. First, Eq. (5) is solved numerically. Then it is possible to utilize Eq. (8) directly in the closed form.

As for the previous category, most results are available in graphic form and the experiments were partitioned into three groups, O, O_g, and O_b by means of analogous considerations. Only three works, 89GER/PIC (OGB), 91SCH/HAR (Oc5, Oc6, Oc7, Oc9, OcB, OcD), and 92MAT/JAC (Om7, OmB, OmF, OmJ, OmN, OmQ) have given the numerical values (group O) and their results are shown in Figs. 6 and 7.

89VER/BRU (N1–N7) made a special apparatus based on the volumetric approach to maintain constant the value of index z while heating or cooling $YBa_2Cu_3O_{6+z}$. As a result, they have managed to obtain results in the form of $\{\ln p(O_2)_{ij}, T_{ij}, z_i\}$. The computation of $p(O_2)_{ij}^{\text{calc}}$ here is analogous to that in the case of isotherms. The results are shown in Fig. 8.

A different experimental path has been implemented by 94TAR/GUS (VT1–VTG) during the traditional volumetric experiment. The total pressure was measured as a function of temperature at constant total volume. After assuming that the gas phase contains molecular oxygen only, the experimental points look like $\{\ln p(O_2)_{ij}, T_{ij}, V_i, z_i'', m_i''\}$, where V_i is the volume of the chamber, z_i'' is the index, and m_i'' is the mass of the original sample. During the experiment, index z changed because some oxygen escaped from $YBa_2Cu_3O_{6+z}$ to the gas phase. Assuming that molecular oxygen obeys the perfect gas law and neglecting the volume of the condensed phase, the current index z_{ij} can be estimated from

$$z_{ij} = z_i^o - 2p(O_2)_{ij}^{\text{calc}} V_i \{M(YBa_2Cu_3O_6) + M(O_2) z_i^o\}/(RT_{ij} m_i^o). \quad (24)$$

Computing $p(O_2)_{ij}^{\text{calc}}(T_{ij}, V_i, m_i^o, z_i^o)$ is a bit more difficult. To achieve this end, one has to solve a system of three equations, (5), (8), and (24) for three unknowns, $\ln p(O_2)_{ij}^{\text{calc}}$, index z and the equilibrium order parameter x. The results will be discussed in Sec. 5.

Oxygen partial enthalpies [see Eq. (19)] have been measured by reaction microcalorimetry in 89GER/PIC (PG) as a function of index z at 873 K, i.e., we have experimental points in the form of $\{\Delta_{ox}H'_{O,ij}, z_{ij}, T_i\}$. Computing $\Delta_{ox}H'^{\text{calc}}_{O,ij}$ is rather straightforward. The results are in Fig. 9.

89PAR/NAV (PP1, PP2, PP3) have also employed high temperature reaction calorimetry. However, the experiment was carried out differently and the results here are available as transposed-temperatures-drop enthalpies

$$YBa_2Cu_3O_{6+z'}(T') = YBa_2Cu_3O_{6+z''}(T'') - (z'/2 - z''/2)O_2(T''). \quad (25)$$

It is possible to convert the measured enthalpies to the oxygen partial enthalpies but we have preferred to employ them directly in the form of $\{\Delta H_{ij}, z'_{ij}, T'_i, z''_i, T''_i\}$ (see Fig. 10). The use of direct experimental values may look as more difficult procedure but this excludes a lot of ambiguity otherwise introduced during the conversion of the primary experimental results. The enthalpy of Reaction (25),

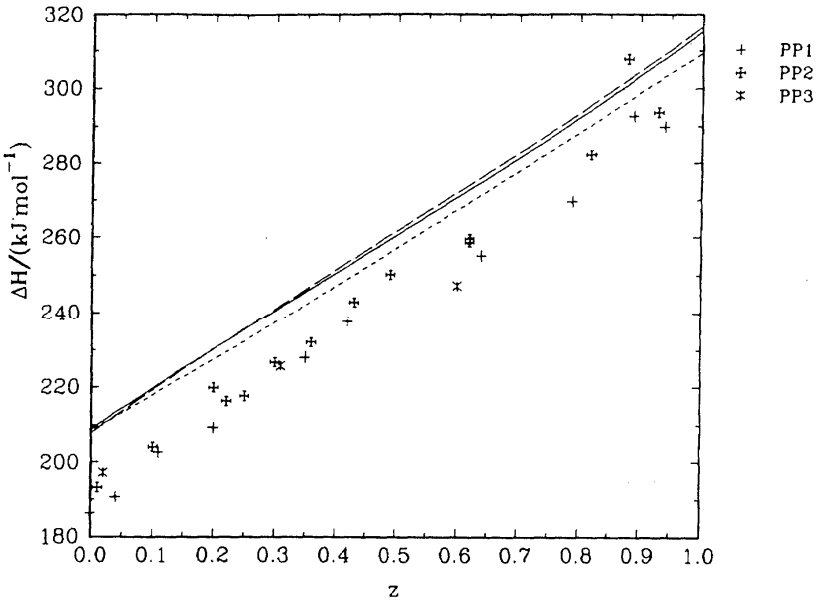

FIG. 10. The enthalpy of Reaction (25) as a function of stoichiometric index z (89PAR/NAV). The solid line is solution ML, the long dashed line is solution WLS, the short dashed line is the solution by 93VOR/DEG.

$\Delta H_{ij}^{\text{calc}}(z'_{ij}, T'_i, z''_i, T''_i)$ can be easily calculated from the enthalpies of $YBa_2Cu_3O_{6+z}$ phase and oxides as follows:

$$\Delta H_{ij}^{\text{calc}} = \Delta_{ox}H(T''_i, z''_i) - \Delta_{ox}H(T'_i, z'_{ij}) + 0.5\{H(T''_i) - H(T'_i)\}_{Y_2O_3} + 2\{H(T''_i) - H(T'_i)\}_{BaO} + 3\{H(T''_i) - H(T'_i)\}_{CuO} + (z'/2 - 0.25)\{H(T''_i) - H(T'_i)\}_{O_2}. \quad (26)$$

3.3. Integral Properties

The measured thermodynamic properties discussed so far would be enough to predict the behavior of the $YBa_2Cu_3O_{6+z}$ phase by itself even though they do not allow us to estimate temperature function $g_1(T)$ in Eq. (2) because it disappears during the differentiation with respect to index z. Yet, in order to predict results of the interaction with other substances one has to know the Gibbs energy as a whole. To

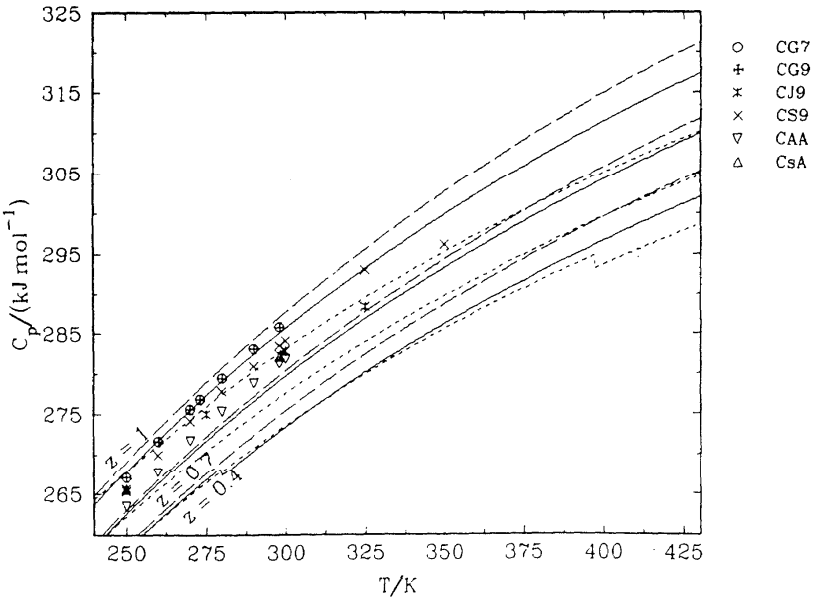

FIG. 11. The heat capacity as a function of the temperature for fixed indices z (adiabatic calorimetry). The solid line is solution ML, the long dashed line is solution WLS, the short dashed line is the solution by 93VOR/DEG. A leap in the heat capacity is due to the tetragonal-orthorhombic phase transition.

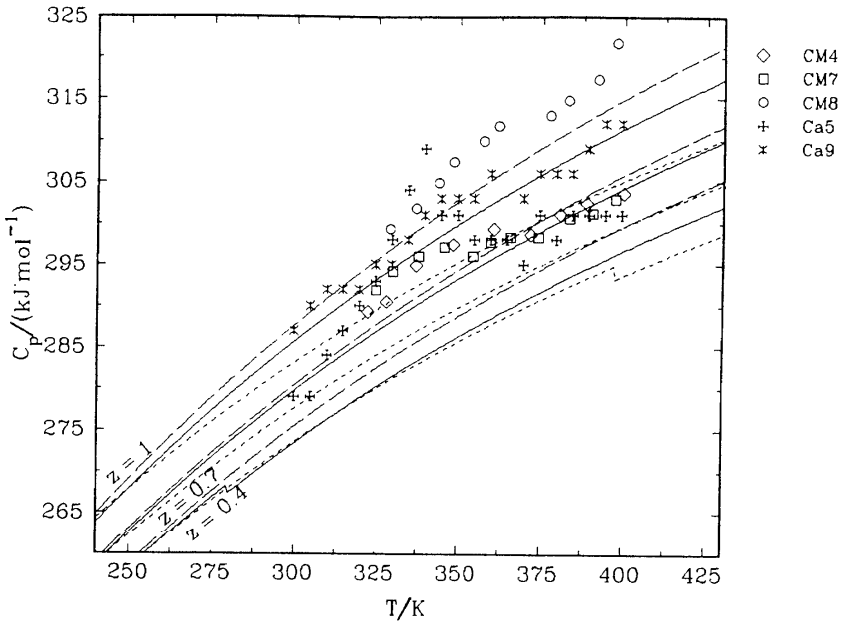

FIG. 12. The heat capacity as a function of the temperature for fixed indices z (DSC). These experimental values have not been included in the final assessment. The solid line is solution ML, the long dashed line is solution WLS, the short dashed line is the solution by 93VOR/DEG.

this end, experiments are available where the integral Gibbs energy, the enthalpy, the entropy, and the heat capacity have been measured.

Oxygen adsorption and desorption from the $YBa_2Cu_3O_{6+z}$ phase below $\approx$450 K can be considered as "frozen" and the index z at these temperatures is not controlled by the external oxygen partial pressure. This allows us to obtain the heat capacity, C_{pz} as a function of temperature at constant z. The experimental point has the form of $\{C_{pz,ij}, T_{ij}, z_i\}$ and the corresponding value of $C^{calc}_{pz,ij}(T_{ij}, z_i)$ can be estimated by Eqs. (16) and (18). All the available values are divided into the two groups: low-temperature heat capacity measured by adiabatic calorimetry (see Fig. 11, Table 2, and Table 3) and high temperature heat capacity measured by differential scanning calorimetry (DSC) (see Fig. 12).

The low-temperature heat capacity measurements are characterized by rather good accuracy and the results are

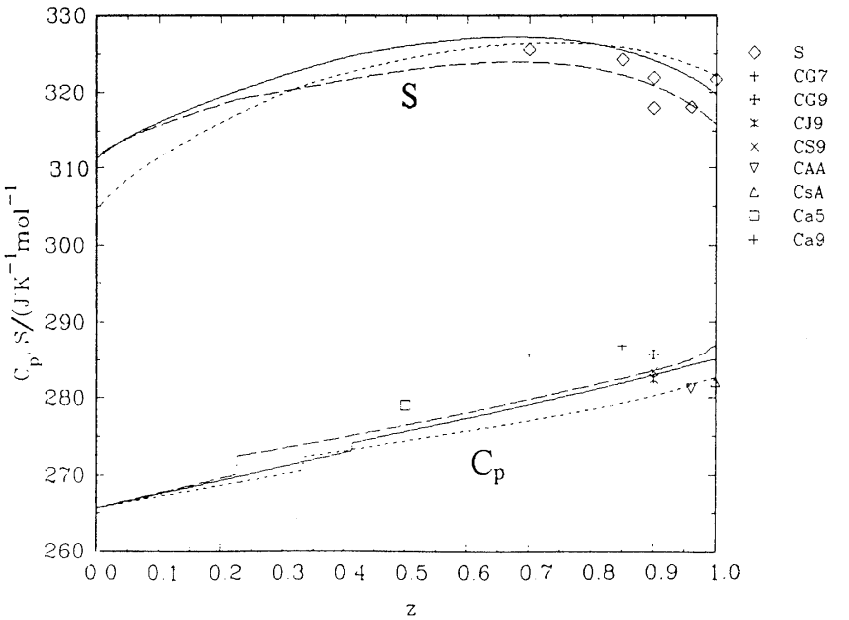

FIG. 13. The entropy and the heat capacity as functions of stoichiometric index z at 298.15 K. The solid line is solution ML, the long dashed line is solution WLS, the short dashed line is the solution by 93VOR/DEG. A leap in the heat capacity is due to the tetragonal-orthorhombic phase transition.

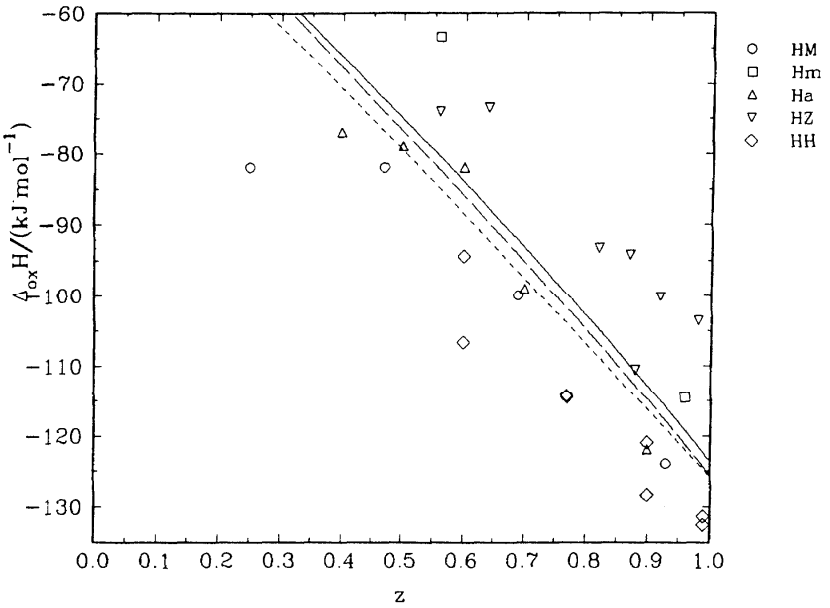

FIG. 14. The enthalpy of formation from oxides as a function of stoichiometric index z at 298.15 K. The solid line is solution ML, the long dashed line is solution WLS, the short dashed line is the solution by 93VOR/DEG.

usually available in the temperature range from liquid helium to room temperature. Because of the limitation of the temperature function accepted in the present work [see Eqs. (20) and (21)] description of the heat capacity was possible only above 250 K. Accordingly, the results of adiabatic calorimetry were employed as two different kinds of measurements, the absolute entropy at 298.15 K, estimated as an integral over all the temperature range, and for the upper part of the heat capacity curve ($T>250$ K). The experimental entropies, $\{S_{ij}, z_{ij}, T_i\}$ are shown in Fig. 13, and Eqs. (15) and (17) show the way how S_{ij}^{calc} can be computed from the model.

The precision of the heat capacity measured by DSC is not as good as from adiabatic calorimetry. Another problem is that at higher temperatures oxygen adsorption/desorption can occur and interpretation of the results becomes rather difficult (see discussion in 93VOR/DEG). This problem was the reason why only high-temperature heat capacities below 425 K were considered in the present work. In the original studies, 90MAT/FUJ (CM4, CM7, CM8) and 91SHA/OZE (Ca5, Ca9), the results are available up to 900 K.

It is impossible to obtain absolute values of the enthalpy and the Gibbs energy, and as was mentioned in Sec. 2, these properties are given for Reaction (3) [see Eqs. (2) and (14)].

The enthalpy of formation of the $YBa_2Cu_3O_{6+z}$ phase has been measured in a number of laboratories by means of solution calorimetry (see Fig. 14 and Table 2) and, as one may expect, there is great scatter among the results. 95MON/POP have thoroughly reviewed calorimetry results and pointed out that the main problem responsible for the scatter between different laboratories is due to impurities of the oxides used for calorimetry (especially BaO that easily reacts with H_2O and CO_2 from the air). Two sets of calorimetry experiments are based on rather a good correlation as follows. If the authors have not paid attention to the purity of the samples or at least this question is not discussed in the article (group H_b), then their results are distinct from those who have carefully discussed this problem (group H). Numerical results for the assessment were taken from 95MON/POP, where almost all results have been recalculated with the same set of auxiliary values.

There are a few papers, 90AZA/SRE (GA), 90FAN/JI (GF), and 91SKO/PAS (GS), giving emf measurements of the Gibbs energy of formation from oxides. Because of the high-temperature nature of the method, the results are available at fixed oxygen partial pressure, i.e., in the form of $\{\Delta_{ox}G_{ij}, T_{ij}, \ln p(O_2)_i\}$ (see Fig. 15). Only the results of 91SKO/PAS are in reasonable agreement with calorimetric enthalpies and entropies ($\Delta G=\Delta H-T\Delta S$). 91VOR/DEG2 have discussed the various works and suggested that the disagreement in the case of 90AZA/SRE and 90FAN/JI can be explained by ambiguities in auxiliary values that are necessary to recalculate the experimental values to Reaction (3). As a result, group G, which, in our view, we can rely upon, contains just 91SKO/PAS and the two other studies are put into the unreliable group G_b.

4. Simultaneous Assessment Under the Linear Error Model

4.1. Formal Task

Formally speaking, the task of simultaneous assessment is to obtain a set of the unknown parameters in Eq. (2) that gives the best description of the original experimental values described in Sec. 3, provided that thermodynamic properties of the oxides and oxygen are given (see Table 1). In other

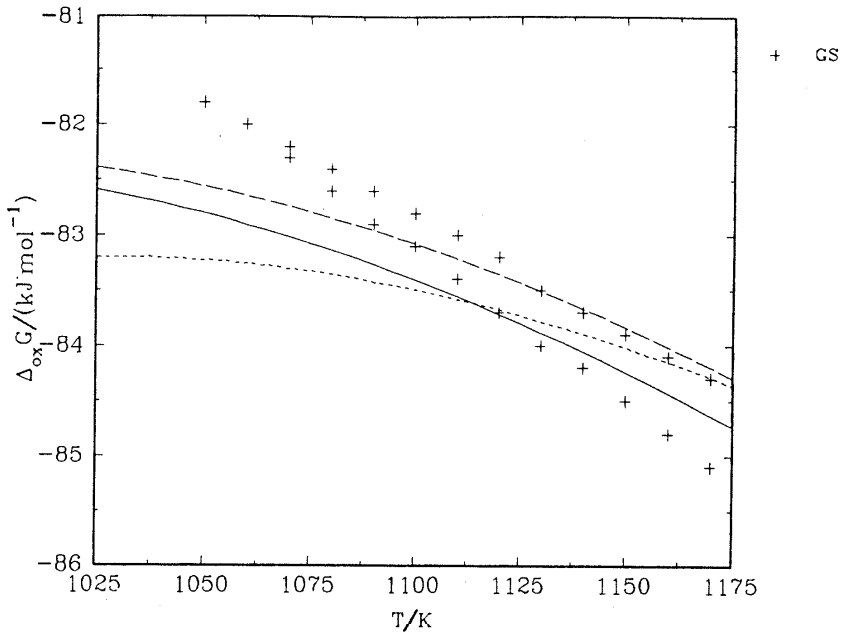

FIG. 15. The Gibbs energy as a function of the temperature for a fixed oxygen partial pressure equal to 1 atm. The solid line is solution ML, the long dashed line is solution WLS, the short dashed line is the solution by 93VOR/DEG.

words, the system of equations (23) is to be solved in respect to the vector Θ with the given set of experimental points $\{y_{ij},u_{ij},v_i\}$ [Eq. (22)].

Thermodynamics adds some specifics to this rather general problem. First, the function $y_{ij}^{\text{calc}}\{u_{ij},v_i;\Theta\}$ is different for different experiments in which y_{ij} may mean completely different physical quantities. Second, the unknown parameters are defined in the Gibbs energy function inside the temperature functions $g_i(T),a_i(T),b_i(T)$ [see Eq. (21)]. Most equations are written for other thermodynamic properties that can be derived from the Gibbs energy by means of calculus. Because of that, the set of unknown parameters is the same for all the equations, even though the equations may look quite different. The lattice model also adds its own specifics. That is, most of the functions are not available in closed form and thus the computation is heavily based on numerical analysis.

Although computing $y_{ij}^{\text{calc}}\{u_{ij},v_i;\Theta\}$ and thus solving the system (23) cannot be considered as routine, this is not the issue with the current computer power at hand. The main problem lies in the question of what should be considered as the best description of the experimental points. Actually the number of unknowns in the system (23) is always greater than the number of equations because experimental errors ε_{ij} are also unknown. Therefore, there is an infinite number of solutions and which one should be taken as the best strongly depends on our considerations of errors. This consideration will be referred as the error model and should not be confused with the thermodynamic model taken by itself.

The conventional approach is to employ WLS, i.e., to find such a solution that brings the sum of squares of the errors

$$SS=\Sigma_{ij}\varepsilon_{ij}^2W_{ij}=\varepsilon'\mathbf{W}\varepsilon \tag{27}$$

to a minimum. In matrix notation ε is the vector that comprises all the errors ε_{ij} from all the experiments (with number of elements Σ_iN_i) and $\mathbf{W}$ is the weight matrix that contains weights for each experimental point on its diagonal, $\mathbf{W}=\text{diag}\{W_{ij}\}$.

The problem that has no clear answer in WLS is how to assess the weights. The final solution certainly depends on the accepted weights, and a different set of weights would lead us to a different solution. Consequently, in WLS, the task of simultaneous assessment becomes that of weight assignment. Mathematical statistics gives a guideline such that, in order to obtain a reliable solution, the weight matrix should be proportional to the inverse of the dispersion matrix of the error vector

$$\mathbf{W}=k\mathbf{D}(\varepsilon)^{-1}. \tag{28}$$

The WLS treatment based on Eq. (28) will be referred to below as the strict weighted least squares method. We can proceed from Eq. (28) to WLS if all the errors ε_{ij} are postulated to be noncorrelated (only in this case does the dispersion matrix take the diagonal form) and ratios between variances for all the errors are known *a priori*. Unfortunately, both statements are too restrictive for real-life applications. The variance ratio for experimental points is not known and there is clear evidence that at least some errors are correlated between each other because of systematic errors. Then, let us start with Eq. (28) and develop a more general approach than WLS.

If variances are not known, the maximum likelihood (ML) method allows us to determine both unknown parameters (vector $\mathbf{\Theta}$) and variances simultaneously by maximizing the likelihood function. This procedure permits us to drop the requirement for variance ratios to be known. Provided all the errors are described by the multinormal distribution, the maximum of the likelihood function coincides with the maximum of (see, for example, 88RAO/KLE)

$$L = -\ln\{\det[\mathbf{D}(\varepsilon)]\} - \varepsilon' \mathbf{D}(\varepsilon)^{-1} \varepsilon. \tag{29}$$

If the error distribution is unknown, finding the maximum of Eq. (29) may be viewed as a heuristic procedure that gives not the worst estimates of the thermodynamic parameters and the components of the dispersion matrix (referred below as variance components). Some other methods for this task are also available (see 88RAO/KLE). Note that WLS is a special case of maximizing Eq. (29) when the variance components are known up to a constant factor. That is, the maximum of (29) matches the minimum of (27) provided there are no other unknowns inside the dispersion matrix but the proportionality factor [Eq. (28)].

The linear error model

$$\varepsilon_{ij} = \varepsilon_{r,ij} + \varepsilon_{a,i} + \varepsilon_{b,i}(u_{ij} - u_i), \tag{30}$$

where

$$u_i = (\Sigma_j u_{ij})/N_i \tag{31}$$

has been recently introduced by 96RUD. It is assumed that the total experimental error ε_{ij} consists not only of the reproducibility error $\varepsilon_{r,ij}$, but also of two systematic errors, $\varepsilon_{a,i}$ and $\varepsilon_{b,i}$. Both systematic errors are constant within the ith experiment, but they are assumed to change randomly among different experiments. The first systematic error, $\varepsilon_{a,i}$, accounts for the shift systematic error and second, $\varepsilon_{b,i}$, for the tilt laboratory factor (tilt systematic error). Note that the linear error is a special case of so-called mixed models (see 88RAO/KLE).

The practical reason for introducing two new terms in Eq. (30) is that the results of distinct experiments usually differ more between each other than the internal reproducibility error in a single experiment. Formally speaking, there is a statistically significant difference between distinct experiments, i.e., the ratio of the corresponding sum of squares is more than Fisher's criterion allows. The systematic errors introduced above permit us to treat this situation by means of formal statistical procedures.

Equation (30) was originally designed for one-dimensional tasks, that is, for processing equations with one controlled variable. Fortunately, it can be applied for the $YBa_2Cu_3O_{6+z}$ phase without any change even though functions $y^{calc}\{u,v\}$, that should be considered, are at least two-dimensional. The reason is that all the measurements in the case of the $YBa_2Cu_3O_{6+z}$ phase are made by means of conventional approach where only one variable has been changed within a single experiment. Thus the measurements can be treated as pseudo-one-dimensional. As experimental physical chemistry switches to multidimensional experimental design (modern analytical chemistry appears to be doing so), the linear error model may need to be modified.

The linear error model results in the dispersion matrix of experimental errors, $\mathbf{D}(\varepsilon)$, taking the block-diagonal form (see details in 96RUD). Each block corresponds to a single experiment and its elements are functions of three variance components,

$$\mathbf{D}(\varepsilon_{r,ij}) = \sigma^2_{r,i}, \quad \mathbf{D}(\varepsilon_{a,i}) = \sigma^2_{a,i}, \quad \mathbf{D}(\varepsilon_{b,i}) = \sigma^2_{b,i}. \tag{32}$$

It is worthy of note that, according to mathematical statistics [see Eq. (28)], weights are related to variances of errors and not to the errors by themselves. In mathematical statistics, an error is considered to be a random quantity with its expected value of zero, and the variance is a property of this random quantity.

The considerations above allow us to set up a task as follows. For the given experimental points $\{y_{ij}, u_{ij}, v_i\}$, it is necessary to determine the vector $\mathbf{\Theta}$ with unknown parameters in the thermodynamic model and unknown variance components contained in the dispersion matrix simultaneously. The ML method provides a framework to achieve this goal and also provides the criterion for the best solution for the system (23). The algorithm for maximizing Eq. (29) under the linear error model given by Eq. (30) is described by 96RUD. Once more, WLS is a special simplified case of the new general task that can be reached by equating the variances of systematic errors (and hence the systematic errors by themselves) to zero and supplying the ratio between variances of the reproducibility error *a priori*.

4.2. Expert Conclusions

Let us stress the difference between experimental errors that can be treated statistically and mere mistakes of experimenters. If the expert conclusion is that there were some mistakes in carrying out the experiment, its results should not be averaged with other experiments because it is not reasonable to average "bad" and "good." In our case, several groups have been discarded before the statistical analysis, based on our informal opinion.

The experiments in groups Z_b, O_b, H_b, and G_b have been presumed to be bad based on comparison with others in the like category (see Sec. 3). During simultaneous assessment, three other groups, T_z, P_b, and V, were found to strongly disagree with the results from different experimental categories and they also were discarded. The question of how to visualize the difference between results in different experimental categories is discussed in Sec. 5. We can speculate that adsorbed gases were responsible for high total pressures at lower temperatures measured by 94TAR/GUS (group V, see also Sec. 5) and that the indirect nature of the values presented in group T_z led to a shift of about 200 K in the temperature of tetragonal-orthorhombic transition (see Fig. 2). Also, we cannot say for sure what went wrong in the experiment on oxygen partial enthalpy by 89GER/PIC (group P_b), but the shape of the curve obtained (see Fig. 9) is in strong disagreement with our model and with the results in groups P and H (Fig. 10 and Fig. 14).

It should be stressed once more that the results of groups Z_b, O_b, H_b, G_b, T_z, P_b, and V are in strong disagreement with the experiments included in the simultaneous assessment. If any experiment discarded by us happens to be a "true" one, then the results obtained in the present work would need to be reconsidered.

Three more groups, Z_g, O_g, and C_h, were also not included in the final assessment, even though the results there are in reasonable agreement with the recommended solution. This means that the final solution does not depend strongly on whether these groups are included or not. There were several reasons to exclude groups Z_g and O_g from the simultaneous assessment. First, the accuracy of the results that were scanned from the figures are difficult to estimate because is not clear how accurately these figures have been made (it is difficult to treat statistically errors made by the illustrator). Second, we believe that authors who fail to supply the results in a form readily useful to others should be somewhat punished (luckily we can afford this in the case of the $YBa_2Cu_3O_{6+z}$ phase). Generally speaking, the $YBa_2Cu_3O_{6+z}$ phase is a very good example of the statement made by the IUPAC commission: "All will have had experience of cases when it has not been possible to decide on the relative merits of conflicting data because of insufficient reporting of uncertainties. Thus, years of work may be rendered useless by the failure of the authors to present his results fully or perhaps by failure to battle with editors for the essential space" (81OLO/ANG). Finally, inclusion of these groups in the assessment made the statistical assumptions below much more complicated.

The reason for excluding group C_h was mostly for cosmetic reasons. If the results of this group are included in the assessment the description of the low-temperature heat capacities obtained by adiabatic calorimetry (we believe that they are more accurate) becomes a bit "tilted."

Thus far there are no differences between WLS and the new ML approach described in the previous section. The difference begins in the next step, where it is necessary to ascribe weights to the experimental points that have been included in the simultaneous assessment.

In order to utilize either WLS or ML, some hypotheses must be formulated about the error dispersion matrix. Note that because of Eq. (28), the terms "dispersion matrix" and "weight matrix" are considered essentially as synonyms in the present work. In some assessments the weights are just chosen by the expert opinion without any use of Eq. (28). We will call this the informal weighted least squares method. In this case, the expert has to specify the numerical values of the weights (the ratios between variances) for all the experimental points. This process usually takes a lot of meditating. The statement "this work is better than that one" is relatively easy to make but the numerical assertion "this work is better by two and half times that that one" is certainly not that straightforward for a human being.

The ML allows the expert to limit himself to qualitative conclusions only. The expert sets the structure of the error dispersion matrix; all the numerical values are estimated by maximizing the likelihood function. Let us see how this idea was implemented in the present work.

First, all the experiments were divided into groups of the same nominal quality, as was discussed in Sec. 3 (see Table 3) and some groups were discarded, as explained above. Certainly, some meditating was inevitable during this process, but because of the qualitative nature of this procedure, the considerations can be better defined and justified than in the informal weighted least squares process. Our final expert conclusion was that we have ten miscellaneous groups of experiments (T_z, X, Z, O, N, P, S, C, H, G) and that all seem to have about the same quality.

Now it is necessary to express this statement in a formal manner. First, the variance of the reproducibility error can be assumed to be the same within each group, giving ten unknown variances. The statement regarding the similar quality of the experiments in these groups cannot be applied to the reproducibility variances because we cannot ever assert that there is any relationship between the reproducibility variances in different data groups.

The problem now is that the experimental uncertainties of the values that have been put into the assessment cannot be described simply by their reproducibility errors. If we put the solution within the reproducibility error for one group then it certainly will go beyond the reproducibility error for another group. Equation (30) allows us to make the next step and to incorporate this fact by introducing the systematic errors and to reformulate the statement of the same quality for the different groups as the principle of like compromise. This principle is that the two ratios

$$\gamma_{a,i}=\sigma_{a,i}^2/\sigma_{r,i}^2, \quad \gamma_{b,i}=\sigma_{b,i}^2/\sigma_{r,i}^2 \tag{33}$$

are assumed to be the same for all the groups included in the simultaneous assessment. To clarify this principle, let us start with the first ratio, $\gamma_{a,i}$.

Under the linear error model, the total error is considered to consist of three terms. The first is the reproducibility error, the second is the shift systematic error, and the third is the tilt systematic error. The second error term allows us to model the calibration error, as now one can say that the experimenter has made a constant error for all the points in this experiment. Then during the measurement procedure the reproducibility error was added at each point. Statistically speaking, both errors are considered to be random but they are characterized by different variances, the reproducibility variance and the shift systematic variance. The shift systematic variance should be different for different groups because it is a dimensional quantity and the data scales are different. However, the ratio $\gamma_{a,i}$ shows the shift systematic variance in relation to the reproducibility variance in the ith group and thus is dimensionless. Then, when we speak about the same quality for the experiments in different groups we imply that the ratio $\gamma_{a,i}$ is the same for these groups.

The situation is analogous with the second ratio, $\gamma_{b,i}$. However there is a small additional problem here because $\gamma_{b,i}$ is still dimensional. The third term in Eq. (30) is similar to the second one in that it is also tied with the systematic

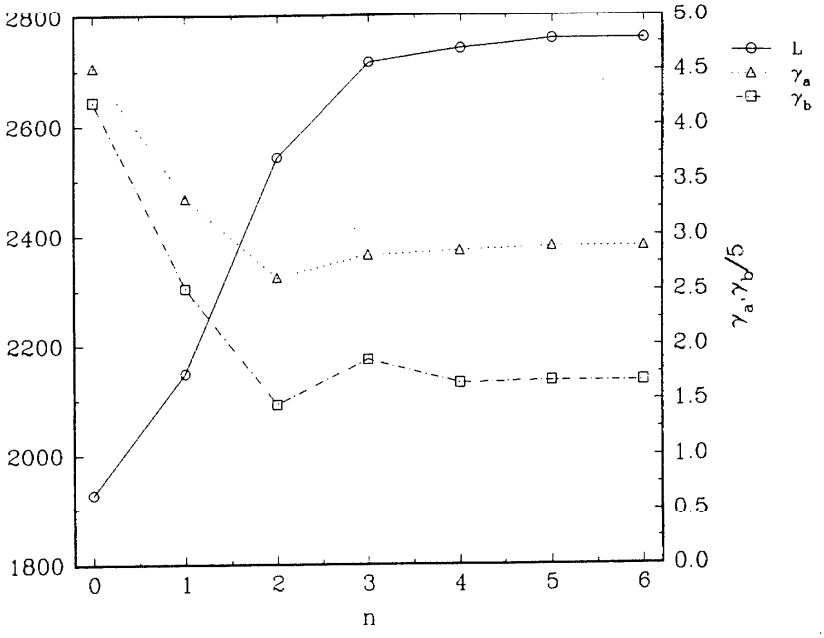

FIG. 16. The dependence of the likelihood function and the ratios, $\gamma_{a,i}$ and $\gamma_{b,i}$ on number of terms in the first sum of Eq. (2).

error, but its nature is different. It is a systematic error that forces the measured curve to tilt from the true behavior. As a result, the tilt systematic variance is associated with the unit length of the controlled variable u, and the ratio $\gamma_{b,i}$ has dimensions equal to the inverse of the u variable. Then, before we say that the ratio $\gamma_{b,i}$ is the same for different groups, it is necessary to compare unit lengths of different controlled variables. This was done by choosing typical ranges of the controlled variable, such as 1000 K for temperature, 10 for $\ln p(O_2)$, and 1 for index z and by somewhat arbitrary equating these ranges between one another.

The assumptions made above give 12 unknowns in the error dispersion matrix [ten for reproducibility variances and two for the ratios in Eq. (34)]. The ML method allows us to leave the variance components as unknowns in the dispersion matrix and to estimate them during the maximization of (29) simultaneously with estimating unknown parameters in Eq. (2).

4.3. Maximizing the Likelihood Function

Another reason for consideration during the simultaneous assessment is a choice of the number of unknown parameters. Actually, Eq. (2) is a series expansion and, before maximizing Eq. (29), the number of terms in the two sums must be defined. The same also concerns Eq. (21) employed in the present work as the temperature function within Eq. (2). A typical solution to this problem is to perform the assessment several times while the number of unknowns is changed. Two criteria have been used to choose the optimal number of unknown parameters: (1) the best description of the experimental points and, at the same time, (2) the conformity of the thermodynamic properties obtained to the general trends of similar materials. Also during the addition of new unknowns, attention has been paid also not to make the whole task ill behaved.

In the previous assessment of 93VOR/DEG, the approximation for the heat capacity, $\Delta_{ox}C_{p,x}=0$ was utilized. This assumption means that just two unknown parameters, A and B, have been left in each temperature function: $g_i(T), a_i(T), b_i(T)$. However, Figs. 12 and 13 show that the experimental heat capacity is higher than predicted by this approximation. Thus, one of the goals in the present assessment was to obtain a better description of the heat capacity. To this end, additional unknowns must be introduced in the temperature functions in addition to A and B. Yet, the number of these additional unknowns happens to be rather limited. It happened to be impossible to put new unknowns in each temperature function because this led to physically unreasonable behavior of the heat capacity.

After many attempts, we decided to introduce new vari-

TABLE 4. The variance components obtained

Group	$\sqrt{\sigma^2_{r,i}}$	$\sqrt{\gamma_a}$	$\sqrt{\gamma_b}$
T_O	11.4 K	2.61	7.19
X	0.0388	2.61	7.19
Z	0.00743	2.61	7.19
O	0.106	2.61	7.19
N	0.156	2.61	7.19
P	4.54 kJ mol^{-1}	2.61	7.19
S	2.51 J·K^{-1} mol^{-1}	2.61	7.19
C	0.813 J·K^{-1} mol^{-1}	2.61	7.19
H	5.01 kJ mol^{-1}	2.61	7.19
G	1.00 kJ mol^{-1}	2.61	7.19

TABLE 5. The parameters within Eqs. (2) and (21) obtained in solution ML[a]

	A	B	C	D
g_1	−3564±541	−4.918±0.490	0	0
g_2	−10360±160	45.99±4.59	−4.051±0.518	−252.3±33.7
a_1	2000±165	−1.544±0.204	0	0
a_2	−2590±224	4.044±0.279	0	0
b_1	652.1±164	3.921±0.193	0	0

[a] g_1, g_2, a_1, a_2, b_1 are the temperature functions within Eq. (2), and A,B,C,D are the parameters within each temperature function according to Eq. (21). The values given lead to the Gibbs energy normalized by the gas constant, G/R. The Gibbs energy can be computed in the temperature range from 250 to 1400 K.

ables C and D in the temperature function $g_2(T)$ only. This means that approximation $\Delta_{ox}C_{px}=0$ has been changed to $\Delta_{ox}C_{px}=k(T)z$. More realistic approximations will be possible after new experimental values on the heat capacity for compositions close to $z=0$ appear.

In the second sum of Eq. (2), only the first term, $b_1(T)$ was left. The unknowns in the second sum depend mainly on the tetragonal-orthorhombic phase transition and occupancies in the oxygen sublattices. One term is enough for the description of these values. Addition of other terms made the task ill behaved.

Figure 16 explains our choice for the number of terms in the first sum of Eq. (2). As the number of terms grows, the maximum likelihood function comes to saturation after sharp rise, and simultaneously, the opposite behavior is found for the ratios, $\gamma_{a,i}$ and $\gamma_{b,i}$. Based on this fact, the use of two terms in the first sum have been presumed to be optimal for the description of the $YBa_2Cu_3O_{6+z}$ thermodynamic properties.

Finally, we have 12 unknown parameters in the Gibbs energy in addition to the ten unknown variance components defined in the previous section. All of them have been determined by maximizing Eq. (29) numerically (see 96RUD for a description of the algorithm). The final values of the variance components are presented in Table 4, and the values of the parameters are in Table 5. Figures 1–15 compare the solutions obtained with the original experimental points.

Figure 17 presents the phase diagram of the $YBa_2Cu_3O_{6+z}$ phase computed from the assessed Gibbs energy. The border between two modifications was calculated by means of Eq. (7) and the miscibility gap by Eq. (13). The phase diagram for a solution of 93VOR/DEG consists from three fields: the tetragonal phase, T, the orthorhombic phase, O, and the miscibility gap, $T+O$, in which the critical point lies on the line of the tetragonal-orthorhombic phase transition. The critical point of the miscibility gap for the ML solution lies within the orthorhombic phase, and thus, the forth field with two orthorhombic phases, $O'+O''$, appears. The phase diagram predicted by the WLS solution will be discussed in Sec. 6.

Some less usual ways of presentation pictures (Figs. 18–27) are discussed in the next sections. Thermodynamic properties of the $YBa_2Cu_3O_{6+z}$ phase are tabulated in Table 6.

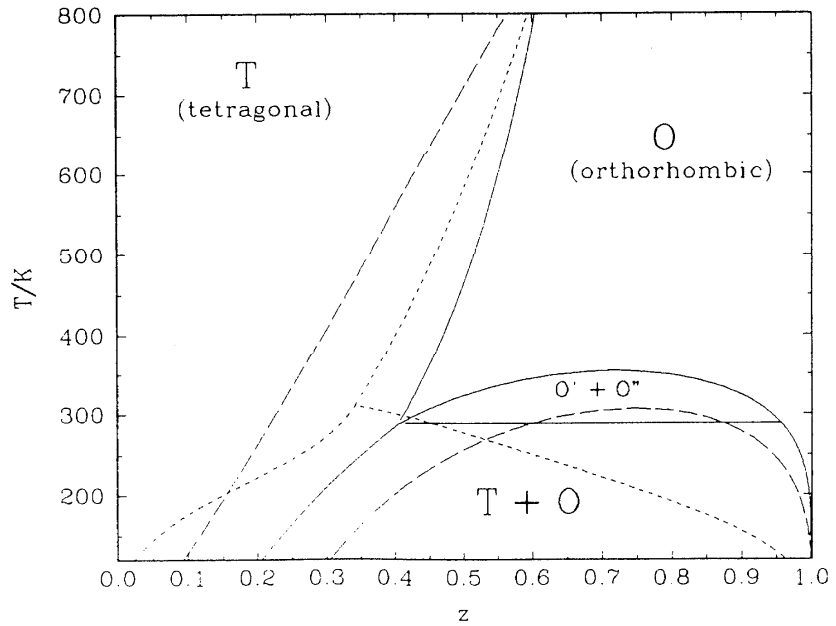

FIG. 17. Phase transformation diagram of the $YBa_2Cu_3O_{6+z}$ phase. The solid line is solution ML, the long dashed line is solution WLS, the short dashed line is the solution by 93VOR/DEG (see Sec. 4.3).

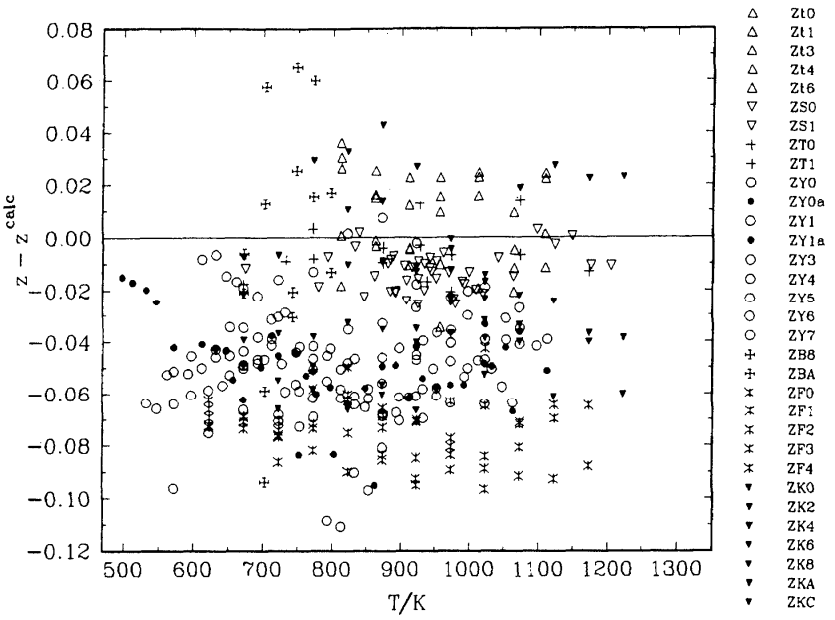

FIG. 18. Deviates for the experiments in group Z_g for solution ML. These experimental values have not been included in the final assessment.

Finally, the correlation matrix for the parameters obtained is given in Table 7. It is important for estimating the variance of the predicted thermodynamic properties at given external conditions. A small program, Y123.EXE, working under Windows 95 and Windows NT to compute thermodynamic properties on the fly, is available from the authors (http://www.chem.msu.su/~rudnyi/Y123/welcome.html).

5. Visualizing the Quality of the Fit

Recently 93ALC/ITK, in their excellent paper devoted to O. Kubaschewski, emphasized the necessity for appropriate display of the measurements in graphical form. We agree completely with 93ALC/ITK that a single statistical criterion cannot replace the analysis of the figures.

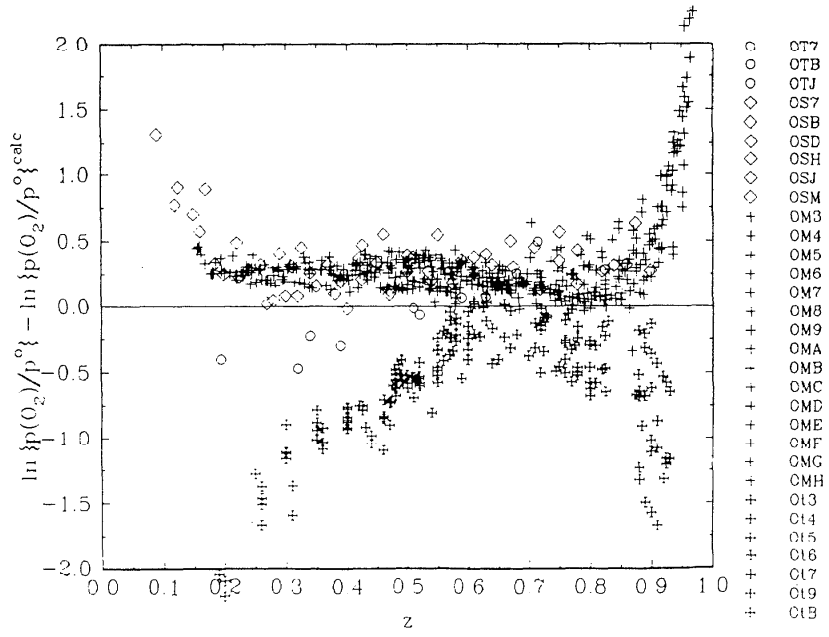

FIG. 19. Deviates for the experiments in group O_g for solution ML. These experimental values have not been included in the final assessment.

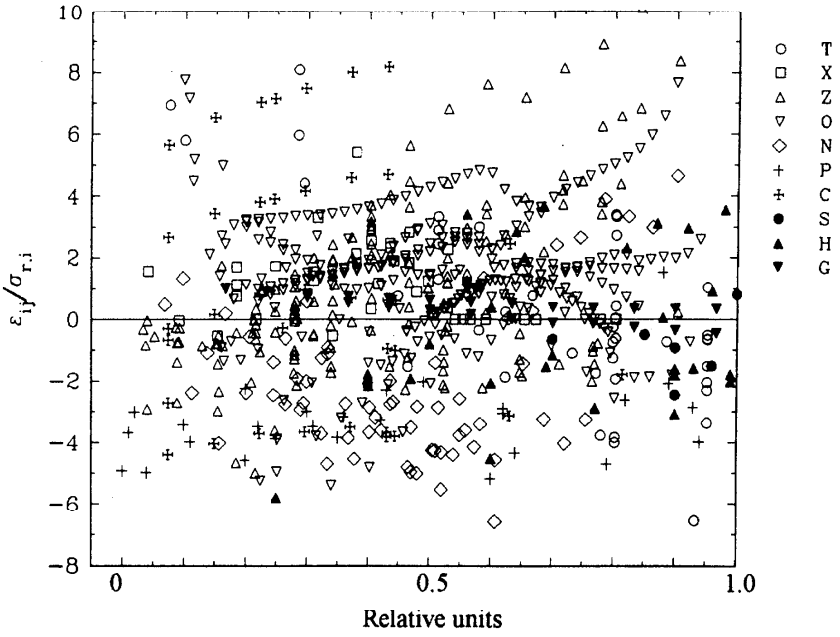

FIG. 20. Normalized deviates for all the experimental points included into the assessment for solution ML.

Figures 1–15 are typical comparisons the fitted curves with the experimental points. The problem is that there is too much data spread among the figures and it would be desirable to provide a digest. Also note that the scale of the figures is low. We can see only large effects, and it is difficult to follow fine details of the data description.

Plotting deviates, i.e., the differences $y_{ij} - y_{ij}^{\text{calc}}\{u_{ij}, v_i; \Theta\}$ allow us to sharply enhance the scale and to put more values on the same graph. Figures 18 and 19 demonstrate this statement with an example of two groups, Z_g and O_g, which were not included in the assessment. Several figures in each group would be required to plot all the experimental points in a reasonable fashion by means of the conventional figures. Note that, because of the enhanced scale, at first glance the scatter may look rather bad, but actually it is about 0.05 in the value of index z and about 0.8

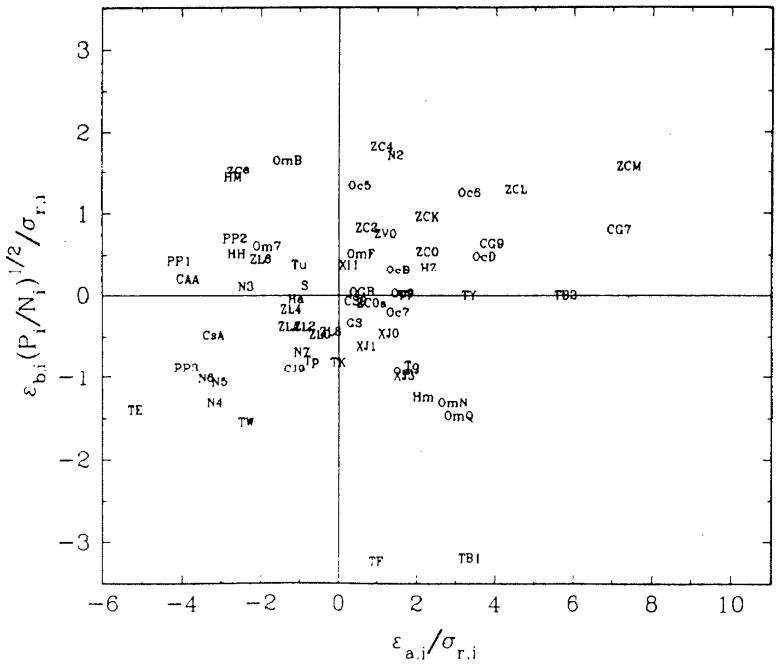

FIG. 21. Tilt systematic error vs shift systematic error for solution ML. The code of the experiment is used as a mark.

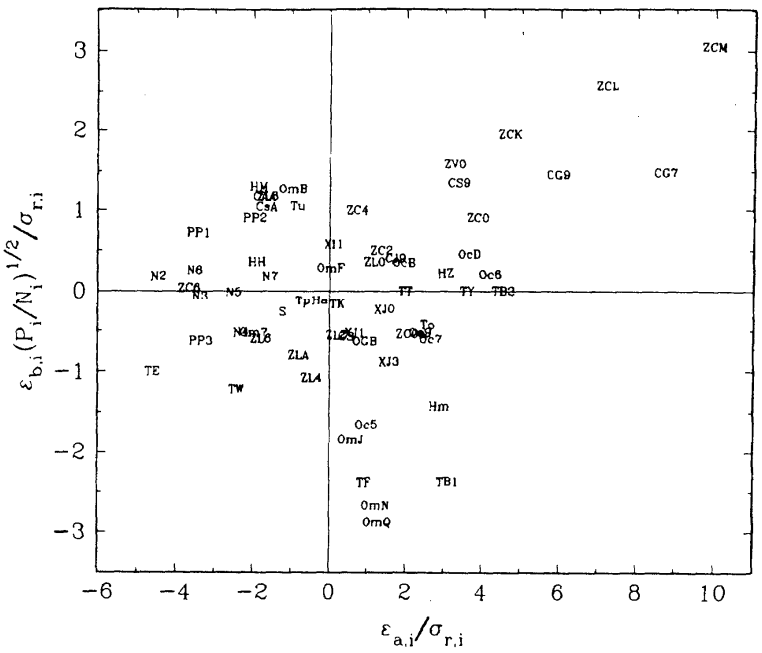

FIG. 22. Tilt systematic error vs shift systematic error for 93VOR/DEG. The code of the experiment is used as a mark.

in the value of $\ln p(O_2)$. The latter value means that the oxygen partial pressures agree within a factor of 2; this is not bad because the absolute value of the oxygen partial pressure varied by six orders of magnitude and the methods employed were rather diverse.

It is possible to go further and to plot deviates normalized by the square root of the reproducibility variance, $[y_{ij} - y_{ij}^{\mathrm{calc}}\{u_{ij},v_i;\Theta\}]/\sigma_{r,ij}$ (see Fig. 20). This display allows us to put the results of heterogeneous experiments on the same figure and to compare them to each other because now the deviates are dimensionless as they are measured by their standard deviation of the reproducibility. Figure 20 is considered to be a statistical portrait of the $YBa_2Cu_3O_{6+z}$ phase because it contains all the experimental points that have been processed simultaneously.

Because of the huge number of experimental points, Figs.

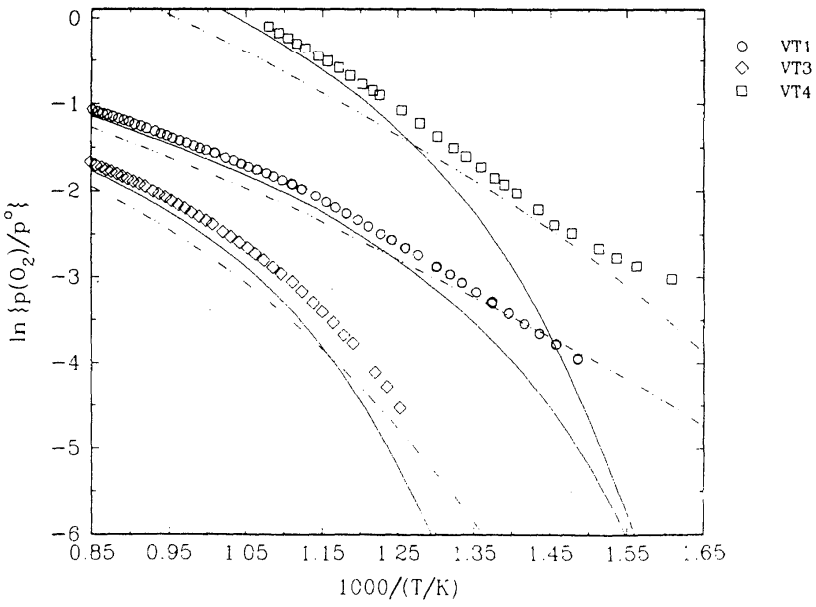

FIG. 23. The total pressure as a function of inverse temperature in 94TAR/GUS. These experimental values have not been included in the final assessment. The solid line is solution ML, the dot dashed line is solution TAR (see Sec. 5).

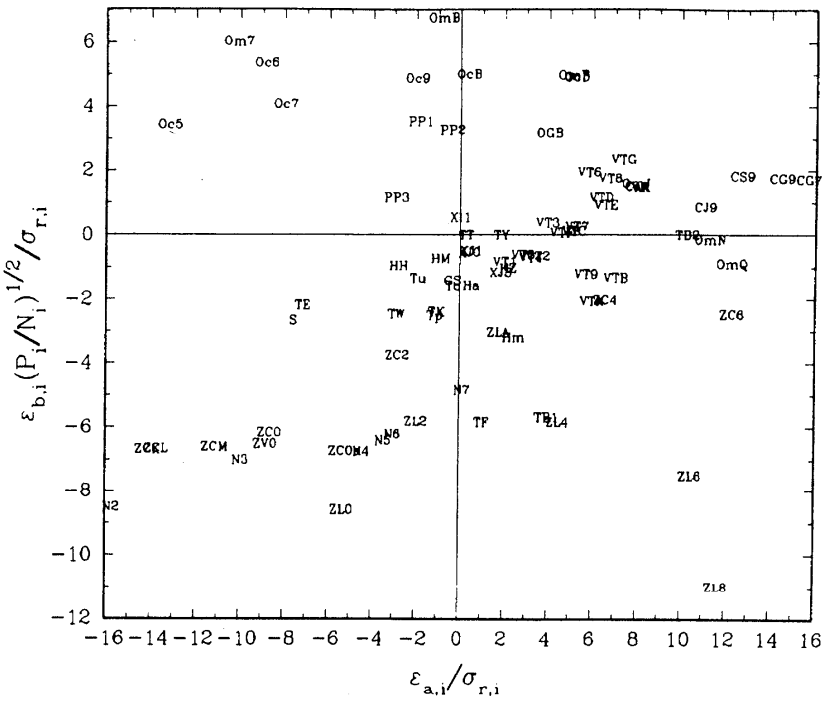

FIG. 24. Tilt systematic error vs shift systematic error for solution TAR. The code of the experiment is used as a mark (compare with Fig. 21, see Sec. 5).

18–20 are rather cluttered. It is difficult to find a particular experiment. Figure 20 is of more esthetic than practical value (especially when it is in color). The linear error model suggests a new type of the graph where each experiment is represented by a single point. The idea is that a typical behavior of the deviates in a single experiment can be described by a line and hence the experimentally measured values are shifted and tilted over the final fitted curve. Hence it is pos-

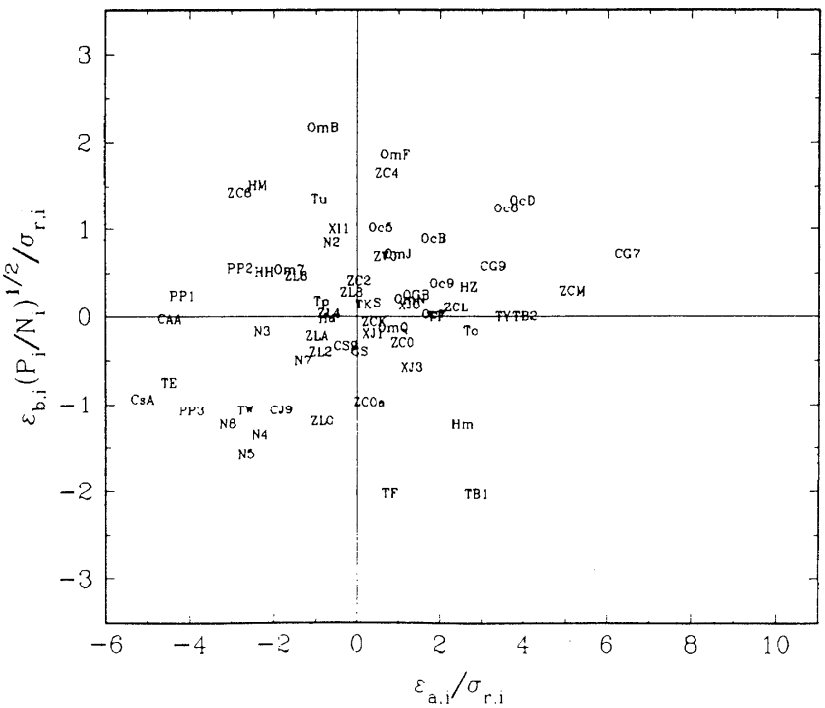

FIG. 25. Tilt systematic error vs shift systematic error for solution WLS. The code of the experiment is used as a mark.

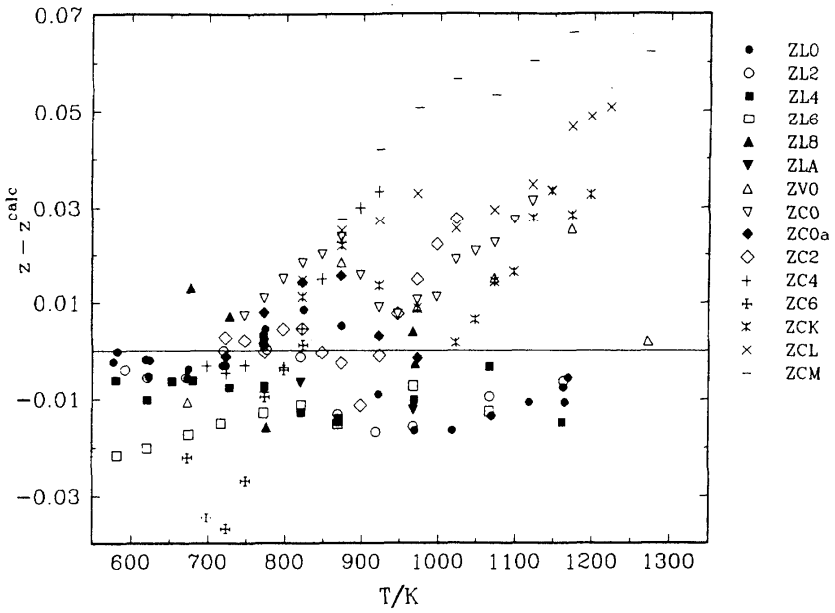

FIG. 26. Deviates for the experiments in group Z for solution ML.

sible to plot the tilt versus shift to see the extent of overall agreement among all the experiments. Again, the tilt and shift is normalized by the standard deviation of the reproducibility to make the comparison of different types of experiments possible. More details about this type of graph are given elsewhere (96RUD, 97KUZ/USP, and 97RUD).

Figures 21 and 22 present this type of the figure for two solutions, recommended in the present work (ML) and from the previous assessment by 93VOR/DEG. These figures give us an overview of the description of all the experiments. It is clearly seen that, in the present assessment, two things have improved considerably: the description of the high pressure results of 92CON/KAR and the heat capacity.

Now let us take the paper of 94TAR/GUS as an example to demonstrate how it is possible to compare different type of experiments during the simultaneous assessment. The problem is that, in the beginning of the assessment, it is not quite clear what experiments agree with each other and which do not. Our approach was to start by including all the experiments, to draw graphs similar to those explained above

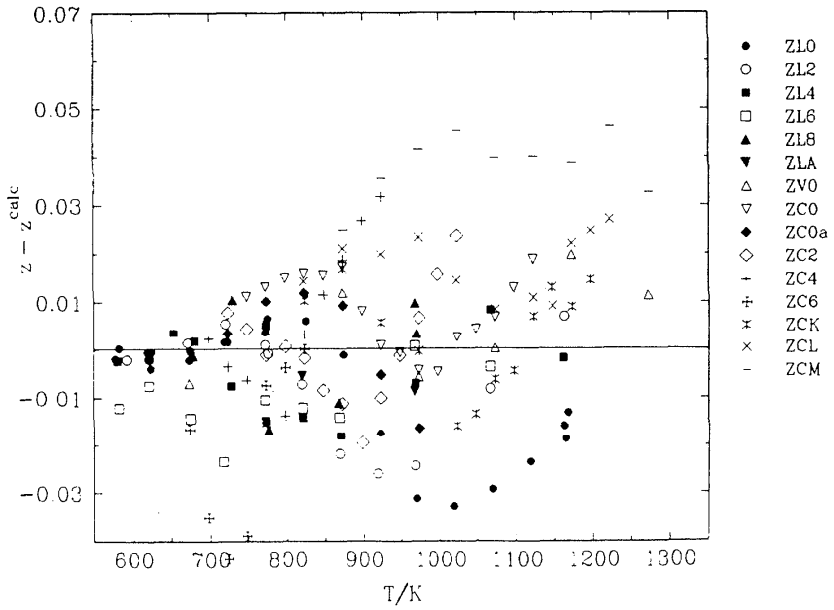

FIG. 27. Deviates for the experiments in group Z for solution WLS.

TABLE 6. Thermodynamic properties of the $YBa_2Cu_3O_{6+z}$ phase[a]

T/K	z	x	C°_{pz} J mol^{-1}K^{-1}	S° J mol^{-1}K^{-1}	$H^\circ - H^\circ_{298}$ kJ mol^{-1}	$\Delta_{ox}H^\circ$ kJ mol^{-1}	$\ln[p(O_2)]/p^o$
298.15	0.00	0.00	265.64	311.10	0.00	−29.63	−∞
300.00	0.00	0.00	266.14	312.74	0.49	−29.63	−∞
400.00	0.00	0.00	287.66	392.48	28.26	−29.63	−∞
500.00	0.00	0.00	302.12	458.32	57.79	−29.63	−∞
600.00	0.00	0.00	312.62	514.38	88.56	−29.63	−∞
700.00	0.00	0.00	320.66	563.20	120.24	−29.63	−∞
800.00	0.00	0.00	327.08	606.45	152.63	−29.63	−∞
900.00	0.00	0.00	332.34	645.29	185.61	−29.63	−∞
1000.00	0.00	0.00	336.77	680.54	219.07	−29.63	−∞
1100.00	0.00	0.00	340.55	712.82	252.94	−29.63	−∞
1200.00	0.00	0.00	343.84	742.59	287.17	−29.63	−∞
298.15	0.25	0.00	270.14	320.85	0.00	−53.01	−54.04
300.00	0.25	0.00	270.66	322.52	0.50	−53.01	−53.60
400.00	0.25	0.00	293.29	403.72	28.78	−52.87	−35.75
500.00	0.25	0.00	308.57	470.90	58.92	−52.64	−25.13
600.00	0.25	0.00	319.70	528.20	90.36	−52.36	−18.14
700.00	0.25	0.00	328.25	578.15	122.77	−52.04	−13.21
800.00	0.25	0.00	335.07	622.44	155.95	−51.67	−9.57
900.00	0.25	0.00	340.68	662.24	189.75	−51.28	−6.79
1000.00	0.25	0.00	345.39	698.38	224.06	−50.86	−4.61
1100.00	0.25	0.00	349.43	731.50	258.80	−50.43	−2.87
1200.00	0.25	0.00	352.93	762.06	293.92	−49.97	−1.45
298.15	0.50	0.16	275.60	326.08	0.00	−75.07	−50.21
300.00	0.50	0.16	276.14	327.78	0.51	−75.07	−49.77
400.00	0.50	0.09	299.75	410.70	29.39	−74.70	−31.94
500.00	0.50	0.00	315.03	479.35	60.18	−74.20	−21.40
600.00	0.50	0.00	326.79	537.88	92.30	−73.64	−14.54
700.00	0.50	0.00	335.84	588.96	125.45	−72.98	−9.72
800.00	0.50	0.00	343.07	634.29	159.41	−72.26	−6.16
900.00	0.50	0.00	349.02	675.05	194.02	−71.47	−3.44
1000.00	0.50	0.00	354.02	712.09	229.19	−70.64	−1.31
1100.00	0.50	0.00	358.31	746.04	264.80	−69.76	0.40
1200.00	0.50	0.00	362.03	777.38	300.82	−68.85	1.79
298.15	0.75	0.34	280.05	326.98	0.00	−98.03	−50.69
300.00	0.75	0.34	280.62	328.72	0.52	−98.02	−50.21
400.00	0.75	0.31	305.39	413.09	29.91	−97.51	−31.06
500.00	0.75	0.29	322.21	483.15	61.34	−96.76	−19.66
600.00	0.75	0.26	334.50	543.04	94.20	−95.85	−12.15
700.00	0.75	0.24	343.96	595.34	128.14	−94.81	−6.86
800.00	0.75	0.22	351.52	641.78	162.93	−93.67	−2.95
900.00	0.75	0.20	357.75	683.55	198.40	−92.45	0.04
1000.00	0.75	0.19	362.99	721.53	234.45	−91.16	2.38
1100.00	0.75	0.17	367.48	756.34	270.98	−89.82	4.27
1200.00	0.75	0.15	371.39	788.49	307.92	−88.43	5.80
298.15	1.00	0.43	285.09	319.68	0.00	−123.50	+∞
300.00	1.00	0.43	285.68	321.44	0.53	−123.49	+∞
400.00	1.00	0.40	311.37	407.41	30.47	−122.80	+∞
500.00	1.00	0.38	328.91	478.88	62.53	−121.80	+∞
600.00	1.00	0.36	341.76	540.04	96.10	−120.58	+∞
700.00	1.00	0.34	351.68	593.50	130.79	−119.20	+∞
800.00	1.00	0.32	359.62	640.99	166.37	−117.69	+∞
900.00	1.00	0.30	366.17	683.74	202.67	−116.07	+∞
1000.00	1.00	0.29	371.68	722.61	239.57	−114.36	+∞
1100.00	1.00	0.28	376.41	758.27	276.98	−112.57	+∞
1200.00	1.00	0.27	380.53	791.20	314.83	−110.72	+∞

[a]T and z are input values, all others including x are computed from the model [Eqs. (2) and (21)] with the values of the parameters listed in Table 5 (see Sec. 2). Note that a value of the order parameter x shows the stable modification of the $YBa_2Cu_3O_{6+z}$ solid solution, x is zero for the tetragonal phase and nonzero for the orthorhombic phase. According to the model, equilibrium oxygen partial pressure is a negative infinite value for the $YBa_2Cu_3O_6$ composition and a positive infinite value for the $YBa_2Cu_3O_7$ composition.

TABLE 7. The correlation matrix for the parameters obtained in solution ML

	$g_{1,A}$	$g_{1,B}$	$g_{2,A}$	$g_{2,B}$	$g_{2,C}$	$g_{2,D}$
$g_{1,A}$	1	-	-	-	-	-
$g_{1,B}$	−0.8456	1	-	-	-	-
$g_{2,A}$	−0.1218	0.1345	1	-	-	-
$g_{2,B}$	0.1600	−0.1655	0.2049	1	-	-
$g_{2,C}$	−0.1588	0.1640	−0.2007	−0.9992	1	-
$g_{2,D}$	−0.1353	0.1394	−0.3648	−0.9787	0.9727	1
$a_{1,A}$	−0.056 36	0.062 41	−0.091 19	−0.2819	0.2870	0.2644
$a_{1,B}$	0.036 00	−0.040 97	0.1732	0.2677	−0.2758	−0.2549
$a_{2,A}$	−0.045 52	0.058 58	0.2790	0.048 80	−0.060 01	−0.05707
$a_{2,B}$	0.044 05	−0.057 68	−0.2795	−0.049 31	0.060 60	0.058 15
$b_{1,A}$	−0.040 51	0.041 31	0.010 65	−0.3108	0.3184	0.2680
$b_{1,B}$	0.044 06	−0.045 75	−0.030 82	0.3079	−0.3148	−0.2641
	$a_{1,A}$	$a_{1,B}$	$a_{2,A}$	$a_{2,B}$	$b_{1,A}$	$b_{1,B}$
$a_{1,A}$	1	-	-	-	-	-
$a_{1,B}$	−0.9832	1	-	-	-	-
$a_{2,A}$	−0.6399	0.6645	1	-	-	-
$a_{2,B}$	0.6637	−0.6948	−0.9926	1	-	-
$b_{1,A}$	0.002 190	0.018 99	0.031 87	−0.050 97	1	-
$b_{1,B}$	0.017 12	−0.044 18	−0.068 32	0.089 11	−0.9914	1

and then to make assessment decisions. During this process we see that the results of 94TAR/GUS are in great disagreement with many papers on the oxygen partial properties. The disagreement can be seen in Fig. 23, where the ML solution is shown with respect to the experimental points. The main difference is at low temperatures where the partial oxygen pressures according to our solution is much lower than measured by 94TAR/GUS. Note that during these experiments the stoichiometric index z changed with temperature and slopes of the curves in Fig. 23 are not connected with the enthalpy of vaporization (compare with Fig. 8).

If we include the results of 94TAR/GUS with nonzero weight, the agreement with their experiments gets much more reasonable (solution TAR in Fig. 23). However the better agreement with 94TAR/GUS means much worse agreement with other experiments that can be clearly seen in Fig. 24 (compare with Fig. 21 and note the difference in scale). For example, the experiments of 89LIN/HUN (ZL0, ZL2, ZL4, ZL6, ZL8, ZLA) in Fig. 24 are seriously shifted and tilted. If we draw the TAR solution in Fig. 4, the difference with the results of 89LIN/HUN would be the same as between the ML solution and experimental points in Fig. 23.

Figure 24 means that, if we presume that 94TAR/GUS is right, then it would mean that many others are wrong, and we have preferred the opposite conclusion. It is worthy of noting that experimental considerations also played not the last role in our conclusion: it may well be that adsorbed gases and not oxygen led to high total pressure at low temperatures in the experiments of 94TAR/GUS.

6. Comparison with Weighted Least Squares

The main difference of the present assessment from the conventional approach lies in introducing the linear error model with two systematic errors. Let us now discuss what practical difference this brought about. To this end, another solution has been found where the variances of systematic errors have been zeroed and the variance of the reproducibility error was assumed to be equal to that obtained in solution ML. This implements the strict WLS method when the weights are equal to the inverse of the reproducibility variances. Note that the reproducibility variances found by the maximum likelihood method under the linear error model should be close to the pooled variance (see 81OLO/ANG) of reproducibility variances for a particular group of experiments. The WLS solution is shown in Figs. 1–15. It is also compared with solution ML in Figs. 25–27.

First, it is possible to state that the description of the original experimental points by both solutions is rather similar. This is in accordance with 96RUD and 97RUD, where it was observed that the conventional treatment may lead to acceptable values of unknown parameters, and that the main difference was in underestimated standard deviations of the parameters by WLS.

In the present work, the overall description is even a bit better for the WLS solution. This can be seen when Fig. 25 is compared with Fig. 21: a circle enclosing experiment marks is a bit smaller in the case of solution WLS. However, there are some subtle effects that allow us to consider solution WLS to be worse in comparison with ML. In the case of the $YBa_2Cu_3O_{6+z}$ phase, it is possible to distinguish between the overall description (for example, the sum of weighted squares) and the description of the function behavior, and our conclusion is that while the former is better for solution WLS, the latter is better for solution ML. Figures 26 and 27 demonstrate this with an example of experiments from group Z. The deviates in group Z are smaller in solution WLS (Fig. 27) than in solution ML (Fig. 26). However the deviates for particular experiments in Fig. 27 possess a systematic S

shape that can be seen for most series. This means that the WLS solution does not follow the shape of experimental points. Therefore, one can say that the function behavior is described better in Fig. 26, even though the overall agreement there is a bit worse. The same can be also said about other groups.

The functional behavior in groups Z and O determine the condition for the tetragonal-orthorhombic phase transition. As a result, we believe that the description of the phase transition is better in solution ML. This belief may be confirmed by looking at the predicted phase diagram of the $YBa_2Cu_3O_{6+z}$ phase (see Fig. 17). The phase diagram that follows from solution ML is rather close to that obtained in the previous assessment of 93VOR/DEG and to what may be expected from structural and theoretical studies (see, for example, 91VOR/DEG). The phase diagram predicted by solution WLS is quite different. The miscibility gap lies completely within the orthorhombic phase and, as a result, the field of miscibility between the tetragonal and orthorhombic phases, T+O, is absent. We believe that it is physically unreasonable.

Pragmatically speaking, solutions ML and WLS differ by variances of systematic errors: these variances were assumed to be zero in the WLS case and were considered to be unknowns in the ML case. This difference in treatment is responsible for the effect described above. When the weights were assigned to the experimental points based on the reproducibility variance in the strict WLS, the number of points in a particular experiment and the range of the controlled variable automatically were used as additional weights when the results of different experiments were processed together.

At first glance, employing the number of experimental points as a weight for otherwise equal conditions seems not to be a bad idea. Yet, if we take into account systematic errors, this approach should be carefully reconsidered. A systematic error is what was constant in a particular experiment. Then, the number of experimental points should not lower the systematic error. Let us imagine that there are two experiments with numbers of points 10 000 and 10, respectively. Provided there were systematic errors that are bigger than the reproducibility error in each experiment, ascribing weights equal to the numbers of points will not lead a good solution. The large number of points leads us to a small reproducibility error of the mean but does not account for systematic error. The systematic errors may be assumed to be of equal magnitude in both experiments, and, because systematic error does not depend on the number of points it would be necessary to average the two means with weights equal to one.

There is no other way in WLS to lessen the number of points in a particular experiment than to switch to an informal WLS approach. Here, the weight is considered to be an expert opinion about the quality of the experiment and Eq. (28) is thrown out. This is always possible but leads to a lot of meditating because the solid ground on which to base a decision is already lost.

The inclusion of the systematic errors in the error model allows us to lessen the effect of differing numbers of experimental points formally because of the block-diagonal structure of the dispersion matrix. After the total error has been separated into the reproducibility error and the systematic errors, the structure of Eq. (29) leads to the following fact. For the likelihood function under the linear error model to reach a maximum, it is more beneficial for the reproducibility variance to be as low as possible, even if this would require some increase in the variances of systematic errors. This characteristic explains why a better description of the function behavior has been achieved in solution ML.

7. Conclusion

The main practical result of the present work is a new set of parameters for computing the Gibbs energy of the $YBa_2Cu_3O_{6+z}$ solid solution, which is the key phase for thermodynamics of the Y-Ba-Cu-O quaternary system. Most results for other phases in this system include equilibria with the $YBa_2Cu_3O_{6+z}$ phase, and thus, the assessment of the whole system depends heavily on thermodynamic values accepted for the $YBa_2Cu_3O_{6+z}$ phase.

Even though the $YBa_2Cu_3O_{6+z}$ phase has attracted a lot of attention in the last decade there are some "blind spots" left. First, there is the area about room temperature where the phase diagram shown in Fig. 17 may well be not quite correct. Recent results (see, for example, 96PIC/GER) suggest the existence of so-called superstructures at these temperatures, and the model employed in the present work does not allow us to describe superstructures at all. Another direction for improvement of the model is the high pressure region (more than 10^8 Pa), where it is impossible to neglect the hydrostatic pressure. At the same time, we believe that the thermodynamic properties at high temperatures and at moderate pressures are well studied now, that our model describes these experimental values adequately, and that this description will not be changed significantly in the foreseeable future.

Besides concrete numbers, there are some methodological points discussed that are of general interest in thermodynamic assessment. Steps to be taken in simultaneous assessment are as follows:

(1) collecting a database of experimental values,
(2) developing a thermodynamic model,
(3) formulating expert conclusion, and
(4) computing unknown parameters and optionally unknown variance components.

Let us see what improvements can be achieved here by employing the linear error model.

First, the whole process cannot be done in a single sequence and in practice the thermodynamic assessment is a somewhat iterative process over these steps until the full satisfaction of the assessor, or probably more often until the time or/and money limit, has been reached. Second, this process cannot be completely formalized and the strategic decisions for the final model and the quality of the experimental

works are always subjective (see 93ALC/ITK for a good discussion on this matter). While keeping this in mind, we enlarge on the last two steps when the model and the experiments to be processed are already chosen.

The starting point for the expert conclusion step is the error model that determines the structure of the dispersion and hence weight matrix. It is the error model that gives a solid background for averaging the experimental values. In the conventional approach, the error model includes just a reproducibility error and, as a result, the weight (dispersion) matrix has the diagonal form. Then an expert has to supply the numerical values of all the weights. Sometimes the expert proceeds from Eq. (28) with the use of some estimates of reproducibility variances, but often she or he just weighs in some manner the quality of experimental points.

However, if we study deviates (see Figs. 18–20, Fig. 26, and Fig. 27) we see that the total error cannot be modeled as the reproducibility scatter only, and this state of affairs is quite common for all the real experimental measurements. The results of a single experiment are not scattered over the fitted curve randomly but rather they are shifted and tilted systematically. If we need reliable results, we have to model this behavior, or otherwise the experimental values will be processed under an incorrect error model.

The linear error model accepted in the present work is a first step in treating the regular behavior of the deviates. It is said that the results are shifted and tilted because of the systematic errors, and, in our view, this is quite conceivable. Definitely, the linear error model is also an approximation of the real picture, and it is possible to introduce more sophisticated error models (see, for example, 88RAO/KLE). Yet, the linear error model allows us to catch the main effects in the trend of the deviates that cannot be ignored, and to leave some more subtle effects to future treatment.

Pragmatically speaking, the linear error model allow us to switch to a nondiagonal dispersion and hence weight matrix. This, in turn, gives us some appropriate tools to influence the number of experimental points in different experiments as discussed in the previous section. The comparison of the two solutions, ML and WLS, shows that, because of treating the systematic errors as the reproducibility errors, WLS have brought a solution where the description of the functional behavior is worse than that in the ML solution.

Another difference between our approach and the conventional one is in estimating variance components. It is possible to say that, in WLS the estimation of the variance components is the expert's responsibility and in our approach they are estimated by means of ML method simultaneously with unknown parameters. This means that expert's work is easier because the expert can express her or his opinion in the qualitative form.

The importance of graphics could not be overestimated. It is impossible to produce a reliable assessment by any method without viewing the agreement between experimental points and the fitted curve in figures. In the present work three types of figures have been employed and from our experience we can state that the best results can be achieved by a combination of all three graph types. Each type shows up its own specific information that is difficult to figure out from another type of graphs.

Finally, the advancement of Internet permits archiving the materials that are necessary for the assessment in the public domain. Our materials including the database of all the experimental values and the optimization software (for Windows 95 and Windows NT) are available from our site, http://www.chem.msu.su/~rudnyi/Y123/welcome.html. After all, if you are not satisfied with our set of parameters you are welcome to make your own.

8. Acknowledgments

The research described in this publication was made possible by Grant No. 96-03-32770 from the Russian Foundation for Basic Research and by Grant No. 96136 from Russian State Program "High Temperature Superconductivity." The authors thank I. A. Uspenskaya for invaluable help during the project and three anonymous reviewers for their useful and helpful comments.

9. References

81OLO/ANG Olofsson, G., Angus, S., Armstrong, G. T., Kornilov, A. N., J. Chem. Thermodyn. **13**, 603 (1981).

85BER/BRO Berman, R. G., Brown, T. H., Contrib. Mineral. Petrol. **89**, 168 (1985).

87BRY/GAL O'Bryan, H. M., Gallagher, P. K., Adv. Ceram. Mater. **2**, 640 (1987).

87EAT/GIN Eatough, M. O., Ginley, D. S., Morosin, B., Venturini, E. L., Appl. Phys. Lett. **51**, 367 (1987).

87FIO/GUR Fiory, A. T., Gurvitch, M., Cava, R. J., Espinosa, G. P., Phys. Rev. B **36**, 7262 (1987).

87JOR/BEN Jorgensen, J. D., Beno, M. A., Hinks, D. G., Soderholm, L., Volin, K. J., Hitterman, R. L., Grace, J. D., Schuller, I. K., Segre, C. U., Zhang, K., Kleefisch, M. S., Phys. Rev. B **36**, 3608 (1987).

87KIS/SHI Kishio, K., Shimoyama, J., Hasegawa, T., Kitazawa, K., Fueki, K., Jpn. J. Appl. Phys., Part 2 **26**, L1228 (1987).

87KUB/NAK Kubo, Y., Nakabayashi, Y., Tabuhi, J., Yoshitake, T., Ochi, A., Utsumi, K., Igarashi, H., Yonezawa, M., Jpn. J. Appl. Phys., Part 2 **26**, L1888 (1987).

87SAL/KOE Salomons, E., Koeman, N., Brouer, R., de Groote, D. G., Griessen, R., Solid State Commun. **64**, 1141 (1987).

87SCH/HIN Schuller, I. K., Hinks, D. C., Beno, M. A., Capone II, D. W., Soderholm, L., Locquet, J. P., Bruynseraede, Y., Serge, C. U., Zhang, K., Solid State Commun. **63**, 385 (1987).

87STR/CAP Strobel, P., Capponi, J. J., Marezio, M., Monod, P., Solid State Commun. **64**, 513 (1987).

87TAK/UCH Takayama-Muromachi, E., Uchida, Y., Yukino, K., Tanaka, T., Kato, K., Jpn. J. Appl. Phys. Part 2 **26**, L665 (1987).

87WU/ASH Wu, M. K., Ashburn, J. R., Tong, C. J., Hor, R. H., Meng, R. L., Gao, L., Huang, Z. J., Wang, Y. Q., Chu, C. W., Phys. Lett. **58**, 908 (1987).

87YUK/SAT Yukino, K., Sato, T., Ooba, S., Ohta, M., Okamura, F. P., Ono, A., Jpn. J. Appl. Phys., Part 2 **26**, L869 (1987).

88GAV/GOR Gavrichev, K. S., Gorbunov, V. E., Konovalova, I. A., Lasarev, V. B., Tishchenko, E. A., Shaplygin, I. S., Izv. AN SSSR, Neorg. Mater. **24**, 343 (1988).

88IEK/NAG Ikeda, K., Nagata, M., Ishihara, M., Kumazawa, S., Shibayama, T., Imagawa, A., Sugamata, T., Katoh, H., Momozawa, N., Umezawa, K., Ihida, K., Jpn. J. Appl. Phys., Part 2 **27**, L202 (1988).

88KOG/NAK Kogachi, M., Nakanishi, S., Nakahigashi, K., Minamigawa, S., Sasakura, H., Fukuoka, N., Jap. J. Appl. Phys., Part 2 **27**, L1228 (1988).

88MEU/RUP Meuffels, P., Rupp, B., Porschke, E., Phys. C **156**, 441 (1988).

88MOR/SON Morss, L. R., Sonnenberger, D. C., Thorn, R. J., Inorg. Chem. **27**, 2106 (1988).

88RAO/KLE Rao, C. R., Kleffe, J., *Estimation of Variance Components and Applications*, North-Holland Series in Statistics and Probability, Vol. 3 (North-Holland, Amsterdam, 1988), p. 370.

88SHE/CHU Sheiman, M. S., Churin, S. A., Kamedova, G. P., Shvetsova, G. K., Nikolaev, P. I., Tezisy dokladov XII Vsesoyuznoi konferentsii po khimicheskoi termodinamike i kalorimetrii (XII All-union conference on chemical thermodynamics and calorimetry, Abstracts), Gorkii, v. 1, p. 140 (1988).

88SPE/SPA Specht, E. D., Sparks, C. J., Dhere, A. G., Brynestad, J., Cavin, O. B., Kroeger, D. M., Oye, H. A., Phys. Rev. B **37**, 7426 (1988).

88TOU/MAR Touzelin, B., Marucco, J. F., J. Less-Common Met. **144**, 283 (1988).

88WAN/LI Wang, H., Li, D. X., Thomson, W. J., J. Am. Ceram. Soc. **71**, C463 (1988).

88YAM/TER Yamaguchi, S., Terabe, K., Saito, A., Yahagi, S., Iguchi, Y., Jpn. J. Appl. Phys., Part 2 **27**, L179 (1988).

89BOR/NOL Bormann, R., Nolting, J., Appl. Phys. Lett. **54**, 2148 (1989).

89BRY/GAL O'Bryan, H. M., Gallagher, P. K., Solid State Ionics **32/33**, 1143 (1989).

89GER/PIC Gerdanian, P., Picard, C., Marucco, J. F., Physica C **157**, 180 (1989).

89GRU/PIV Grunin, V. S., Pivovarov, M. M., Patrina, I. B., Razumeenko, M. V., Bubnova, R. A., Domnina, M. I., Shul'ts, M. M., Dokl. Acad. Nauk SSSR **307**, 143 (1989).

89JUN/ECK Junod, A., Eckert, D., Triscone, G., Lee, V. Y., Muller, J., Phys. C **159**, 215 (1989).

89LIN/HUN Lindemer, T. B., Hunley, J. F., Gates, J. E., Sutton, A. L., Brynestad, J., Gallagher, P. K., J. Am. Ceram. Soc. **72**, 1775 (1989).

89MEU/NAE Meuffels, P., Naeven, R., Wenzl, H., Phys. C **161**, 539 (1989).

89PAR/NAV Parks, M. E., Navrotsky, A., Mocala, K., Takayama-Muromachi, E., Jacobson, A., Davies, P. K., J. Solid State Chem. **79**, 53 (1989).

89TET/TAN Tetenbanm, M., Tani, B., Czech, B., Blander, M., Physica C **158**, 377 (1989).

89VER/BRU Verweij, H., Bruggink, W. H. M., J. Phys. Chem. Solids **50**, 75 (1989).

90AZA/SRE Azad, A. M., Sreedharan, O. M., Supercond. Sci. Technol. **3**, 159 (1990).

90DEG Degtyarev, S. A., Sverkhprovodimost: Fiz., Khim., Tech. **3**, 115 (1990).

90DEG2 Degtyarev, S. A., Sverkhprovodimost: Fiz., Khim., Tech. **3**, 130 (1990).

90FAN/JI Fan, Z., Ji, C. J., Zhao, Z., J. Less-Common Met. **161**, 49 (1990).

90FUE/IDE Fueki, K., Idemoto, Y., Ishizaka, H., Phys. C **166**, 261 (1990).

90MAT/FUJ Matsui, T., Fujita, T., Naito, K., Takeshita, T., J. Solid State Chem. **88**, 579 (1990).

90MER/DEG Merzhanov, I. A., Degtyarev, S. A., Sverkhprovodimost: Fiz., Khim., Tech. **3**, 125 (1990).

90SHA/WES Shaviv, R., Westrum, E. F., Brown, R. J. C., Sayer, M., Yu, X., Weir, R. D., J. Chem. Phys. **92**, 6794 (1990).

91ATA/HON Atake, T., Honda, A., Kawaji, H., Physica C **190**, 70 (1991).

91GAR/RAI Garzon, F. H., Raistrick, I. D., Ginley, D. S., Halloran, J. W., J. Mater. Res. **6**, 885 (1991).

91LEE/LEE Lee, B. J., Lee, D. N. J. Am. Ceram. Soc. **74**, 78 (1991).

91SCH/HAR Schleger, P., Hardy, W. N., Yang, B. X., Physica C **176**, 261 (1991).

91SHA/OZE Sharpataya, G. A., Ozerova, Z. P., Konovalova, I. A., Lasarev, V. B., Shaplygin, I. S., Neorg. Mater. **27**, 1674 (1991).

91SKO/PAS Skolis, Yu. Ya., Pashin, S. F., Kitsenko, S. V., Kovba, M. L., Fomichev, D. V., Tezisy dokladov 13 Vsesoyuznoi konferentsii po khimicheskoi termodinamiki i kalorimetrii (All-union conference on chemical thermodynamics and calorimetry, Abstracts), Krasnoyarsk, v. 1, p. 62 (1991).

91VOR/DEG Voronin, G. F., Degterov, S. A., Physica C **176**, 387 (1991).

91VOR/DEG2 Voronin, G. F., Degtyarev, S. A., Skolis, Yu. Ya., Dokl. Acad. Nauk SSSR **319**, 899 (1991); English translation in Dokl. Phys. Chem. **319**, 565 (1991).

92CHO/KAN Choy, J. H., Kang, S. G., Choi, Q. W., Jung, D. Y., Demazeau, G., Mater. Lett. **15**, 156 (1992).

92CON/KAR Conder, K., Karpinski, J., Kaldis, E., Rusiecki, S., Jilek, E., Physica C **196**, 164 (1992).

92IDE/TAK Idemoto, Y., Takahashi, J., Fueki, K., Physica C **194**, 177 (1992).

92MAT/JAC Mathews, T., Jacob, K. T., Metall. Trans. A **23**, 3325 (1992).

92ZHO/NAV Zhou, Z. G., Navrotsky, A., J. Mater. Res. **7**, 2920 (1992).

93ALC/ITK Alcock, C. B., Itkin, V. P., J. Phase Equilibria **14**, 409 (1993).

93VOR/DEG Voronin, G. F., Degtyarev, S. A., Zh. Fiz. Khim. **67**, 1351 (1993); English translation in Russ. J. Phys. Chem. **67**, 1213 (1993).

93MAT/POP Matskevich, N. I., Popova, T. L., Titov, V. A., Kravchenko, V. S., Shaburova, V. P., Potapova, O. G., Zh. Fiz. Khim. **67**, 1342 (1993).

93PLE/ALT Plewa, J., Altenburg, H., Hauck, J., Z. Metall. **84**, 652 (1993).

93PRI/ZIN Prisedskii, V. V., Zinchenko, O. V., Lotar', E. V., Dokl. Acad. Nauk Ukr. **4**, 130 (1993).

94KIM/GAS Kim, J. S., Gaskell, D. R., J. Am. Ceram. Soc. **77**, 753 (1994).

94MON/POP Monaenkova, A. S., Popova, A. A., Zaitseva, N. V., Bykov M. A., Kovba, M. L., Zh. Fiz. Khim. **68**, 603 (1994).

94TAR/GUS Tarasov, I. V., Gus'kov, V. N., Lazarev, V. B., Neorg. Mater. **30**, 1588 (1994).

95HEN/ZHE Hengzhong, Z., Zheng, F., Pingmin, Z., Xinmin, C., J. Solution Chem. **24**, 565 (1995).

95MON/POP Monaenkova, A. S., Popova, A. A., Zaitseva, N. V., Zh. Fiz. Khim. **69**, 1543 (1995).

96BOU/HAC Boudene, A., Hack, K., Mohammad, A., Neuschutz, D., Neuschutz, D., Zimmerman, E., Effenberg, G., Fries, S., Lukas, H. L., Konetzki, R. A., Schmidt-Fetzer, R., Huang, W., Sundman, B., Bernard, C., Colinet, C., Pasturel, A., Pisch, A., Weiss, F., Rais, A., Ganteaume, M., Mathieu, J. C., Rogez, J., Agrent, B. B., Dinsdale, A. T., Watson, A., High Temp.

Mater. Sci. **35**, 159 (1996).
96PIC/GER Picard, C., Gerdanian, P., J. Mater. Chem. **6**, 619 (1996).
96RUD Rudnyi, E. B., Chemometrics Intel. Lab. Systems **34**, 41 (1996).
97KUZ/USP Kuzmenko, V. V., Uspenskaya, I. A., Rudnyi, E. B., Bull. Soc. Chim. Belges **106**, 235 (1997).
97RUD Rudnyi, E. B., Chemometrics Intel. Lab. Systems **36**, 213 (1997).
97VOR/USP Voronin, G. F., Uspenskaya, I. A., Zh. Fiz. Khim. **71**, 1750 (1997); English translation in Russ. J. Phys. Chem. **71**, 1572 (1997).